

Seafloor age and the evolution of plate tectonic heat transport

Thorsten Becker

University of Southern California

Clint Conrad (U Hawaii)

Bruce Buffett (UC Berkeley)

Sean Loyd (USC)

Lapo Boschi (ETH Zürich)

Bernhard Steinberger (GFZ)

Carolina Lithgow-Bertelloni (UCL)

Brad Foley (Yale)

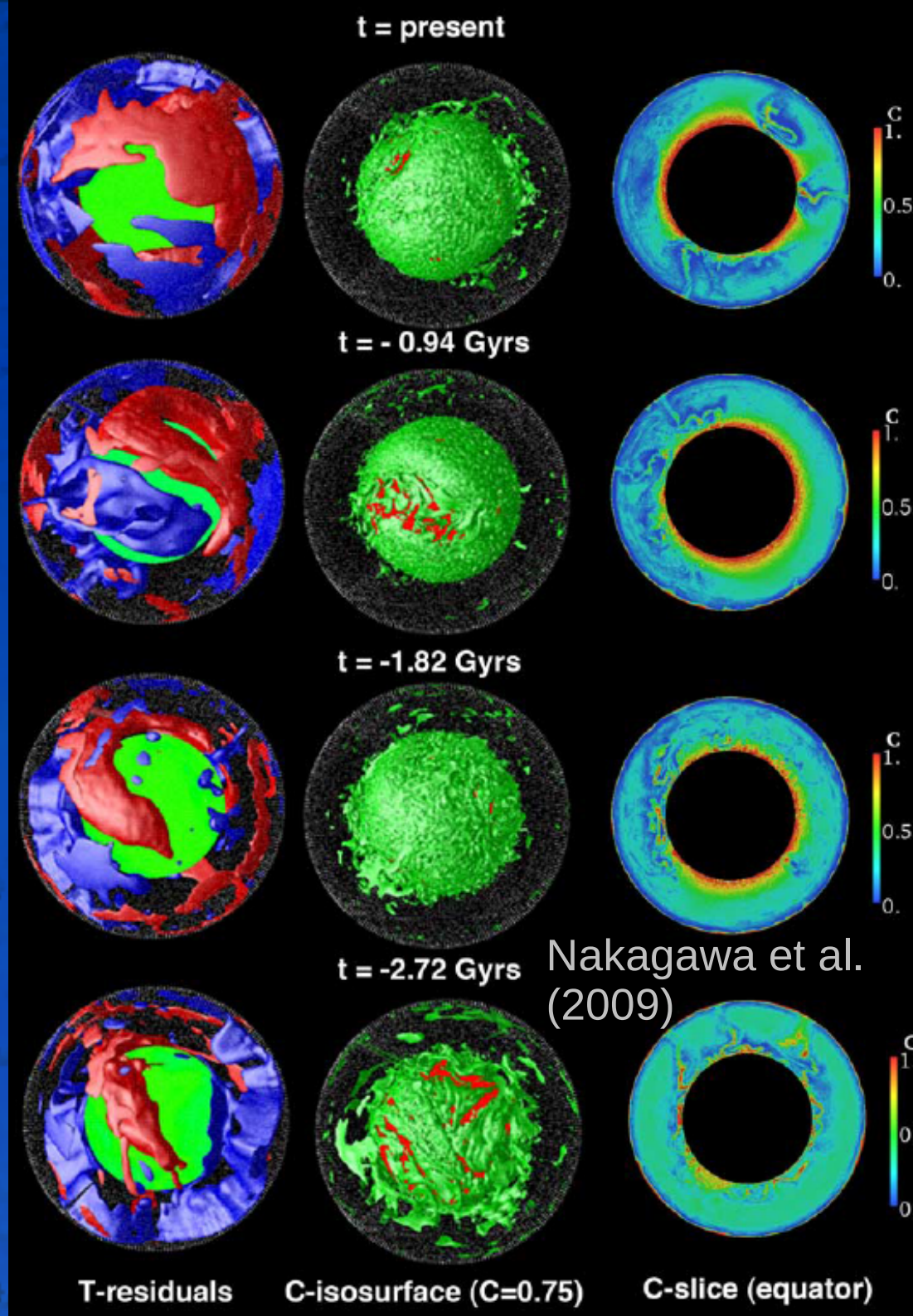
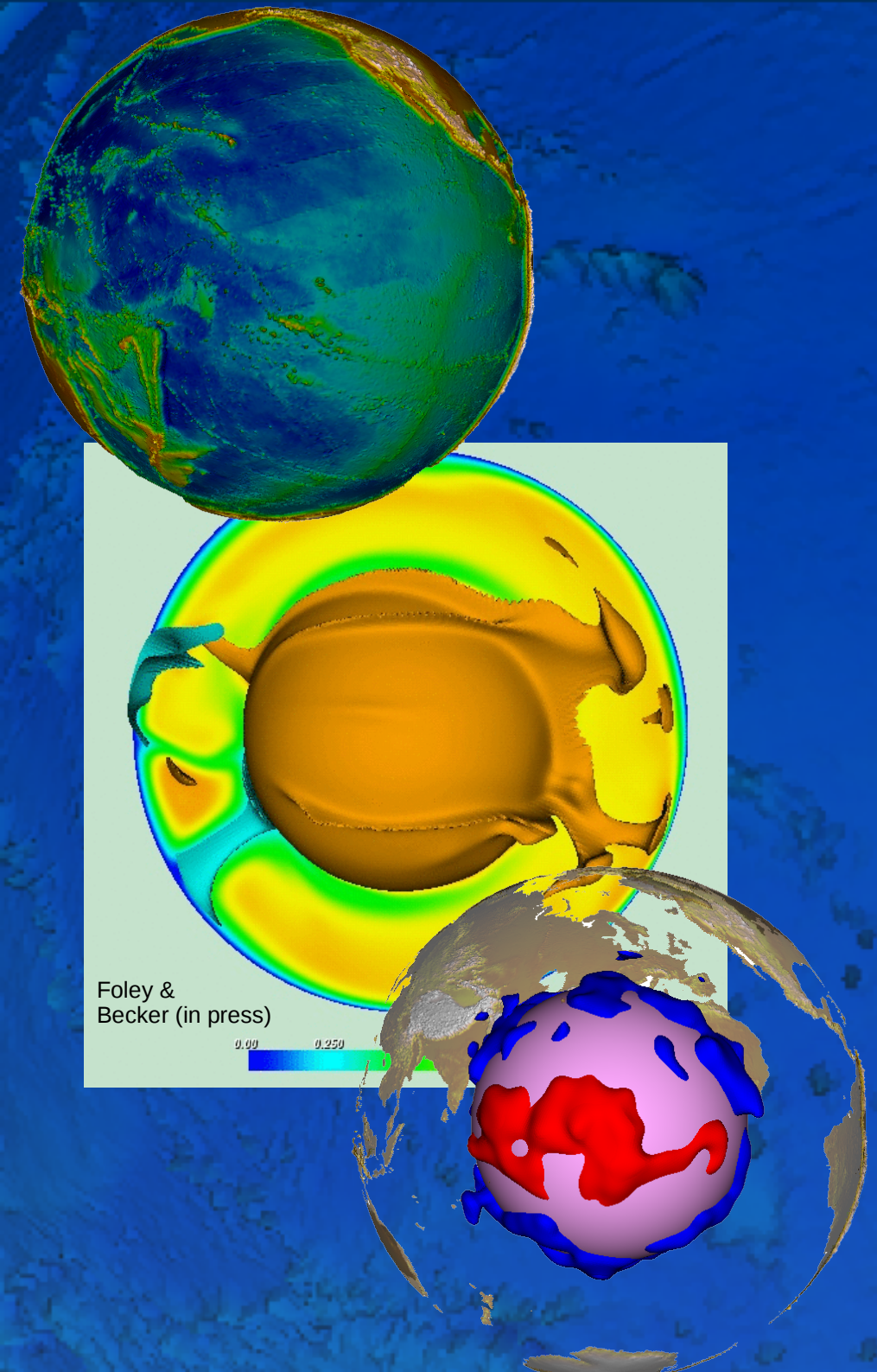
Frank Corsetti (USC)

Dietmar Müller (U Sydney)

11th International Workshop on

Modeling of Mantle Convection and Lithospheric Dynamics

June 30, 2009

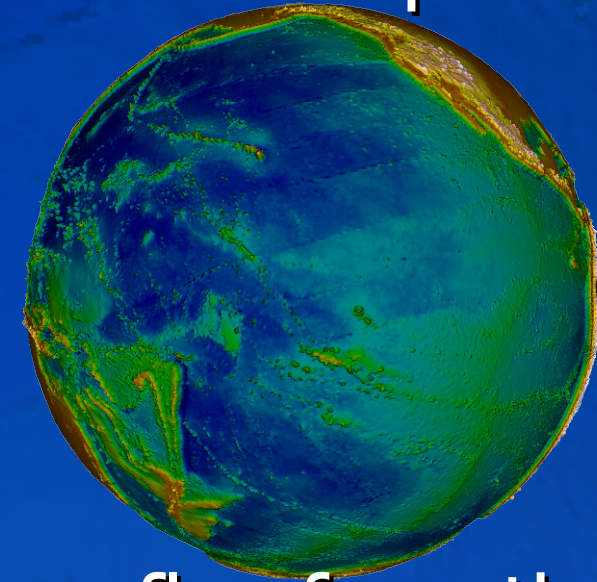
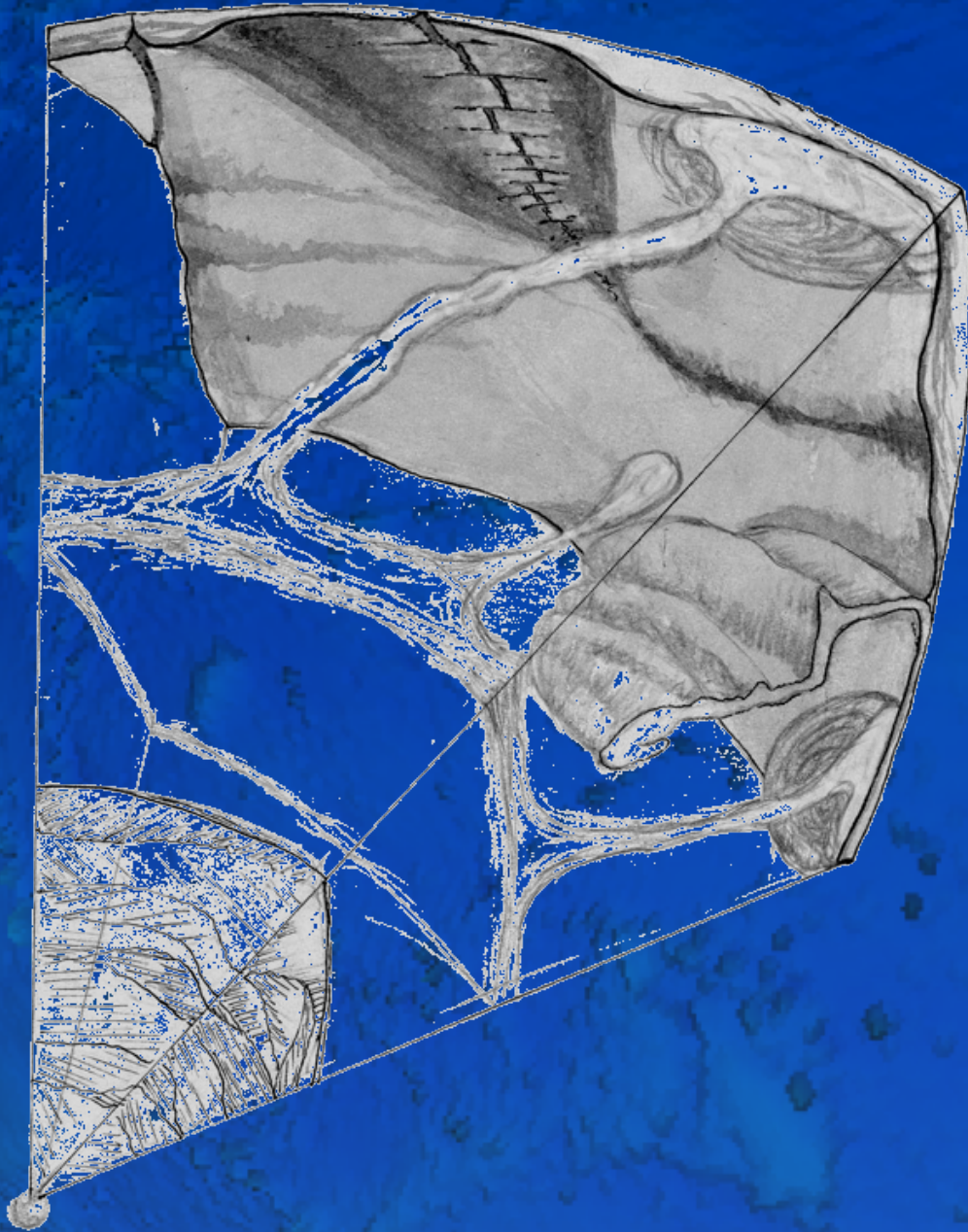


Questions about the mantle system (chemistry and rheology)

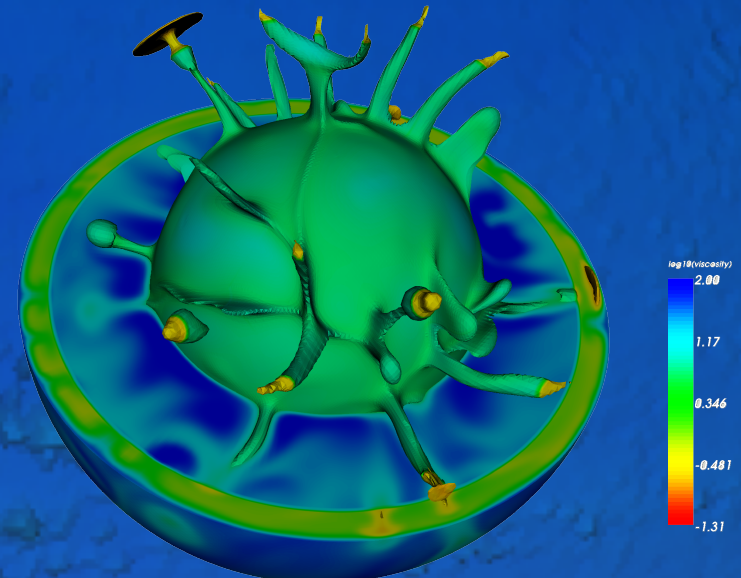
- What causes and controls plate tectonics?
 - Spatial strain localization, memory/damage
 - Why (only) Earth?
 - **Temporally cyclic, uniform, or punctuated?**
- Thermo-chemical evolution of Earth
 - Role of H₂O and C cycling, biosphere
 - Role of continental dynamics
 - **Role of the lower thermal boundary and plumes?**

Mantle heat transport constraints

- Oceanic lithosphere

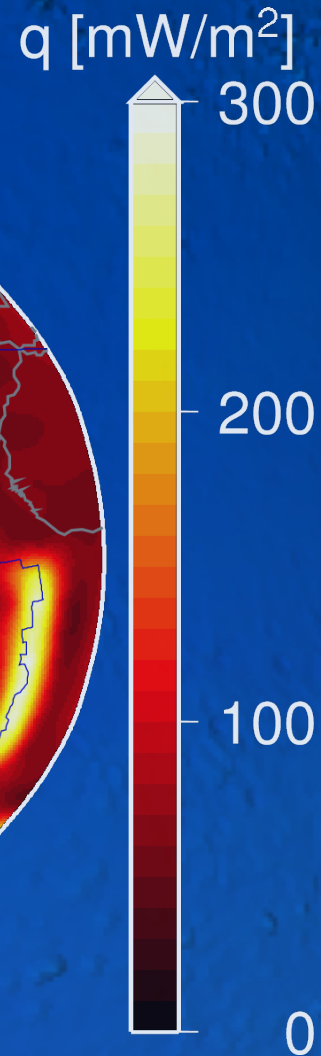


- Plume flux from the CMB

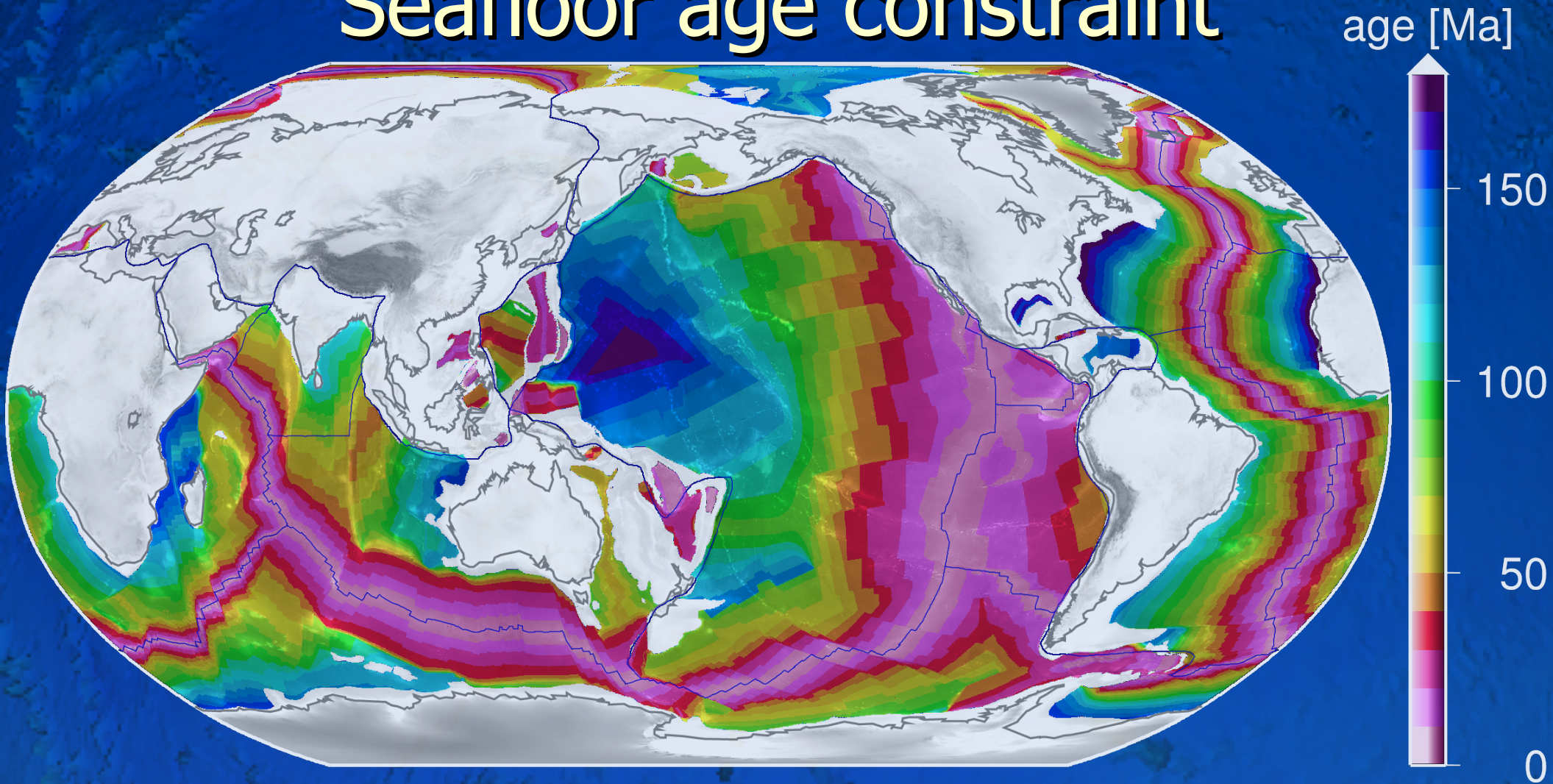


Present day heat budgets

- ~ 44 TW total heat flux
- ~ 8 TW heating by continental crust
- ~ 36 TW for convective heat flux
 - $\sim 70\%$ of heat loss through oceanic lithosphere (i.e. plate tectonics)
 - ~ 3 x radiogenic heating in mantle, i.e. Urey ratio $\sim 1/3$



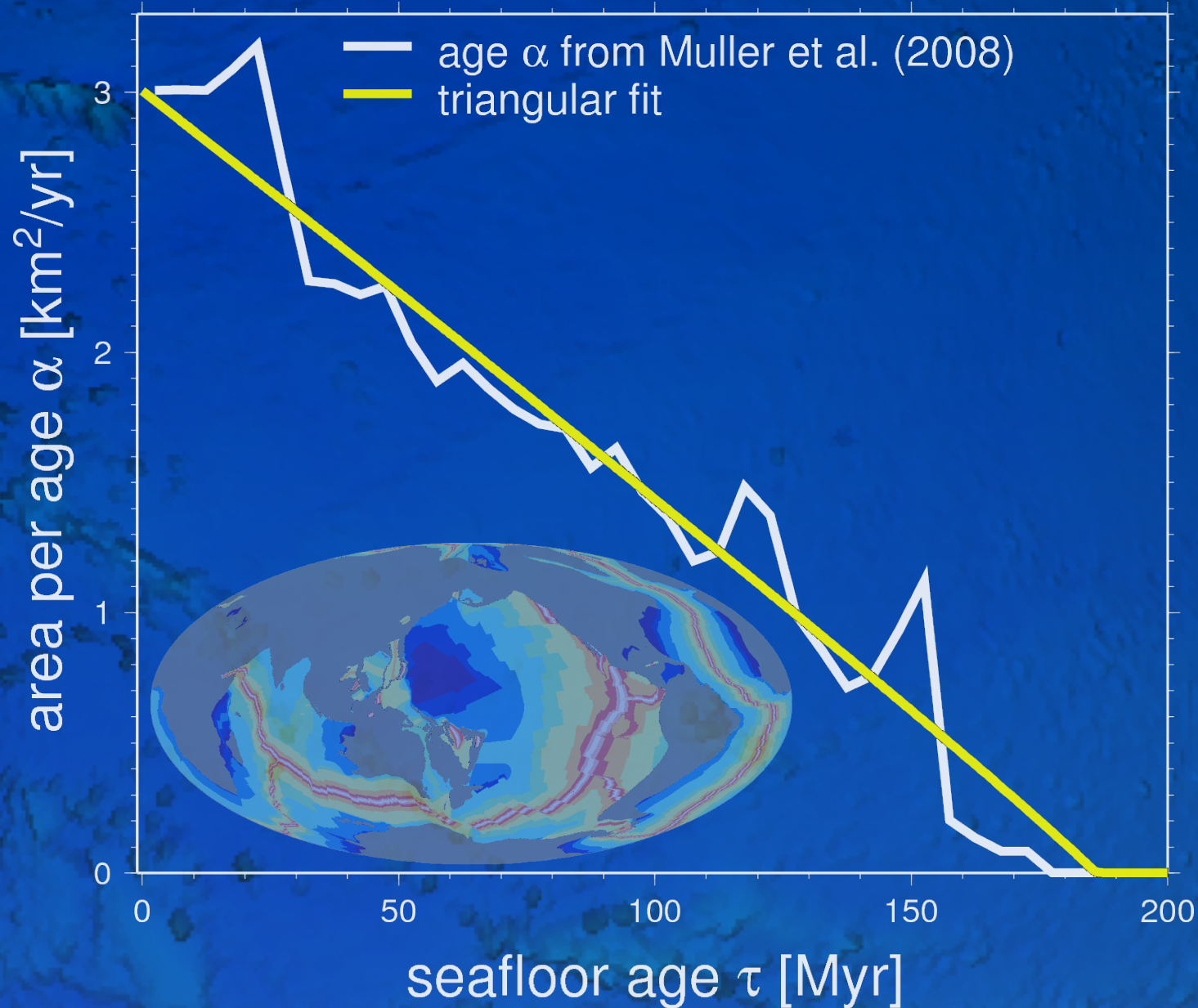
Seafloor age constraint



- Product of plate reorganizations and spreading rate variations
- Besides heat flow, implications for relative sealevel, ocean geochemistry, and ocean circulation

Present-day seafloor age distribution

- Triangular age distribution may indicate
 - Uniform subduction rate, unlike thermal convection (Parsons, 1982)
 - Constant seafloor production since 180 Ma (Rowley, 2002)
- Continents and sphericity will affect age distribution (Labrosse & Jaupart, 2007)



A 1-D model of seafloor age distribution (α) over time

$$\alpha(\tau + d\tau, t + dt) = \alpha(\tau, t) - \Phi(\tau, t) dt$$

- Model equation
 τ = age t = time
 Φ = destruction rate
- Stationary subduction probability ϕ
- Total area constant
 C = production rate
- $\alpha(\tau = 0, t) = C(t)$

$$\frac{\partial \alpha}{\partial \tau} + \frac{\partial \alpha}{\partial t} = -\Phi(\tau, t)$$

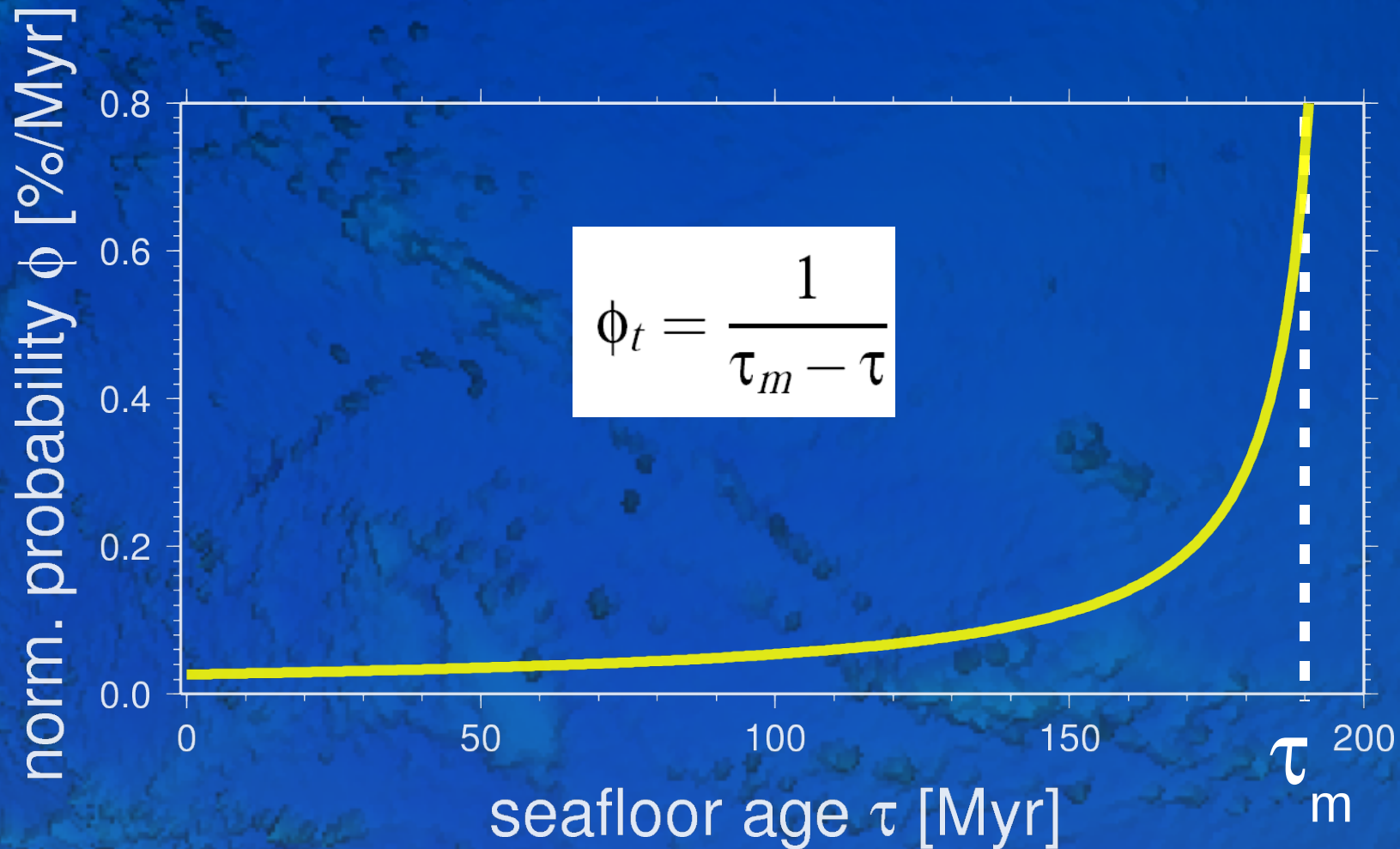
$$\Phi(\tau, t) = \alpha(\tau, t)\phi(\tau)$$

$$C(t) = \int_0^{\infty} \Phi(\tau, t) d\tau$$

Subduction probability for constant production and triangular distribution

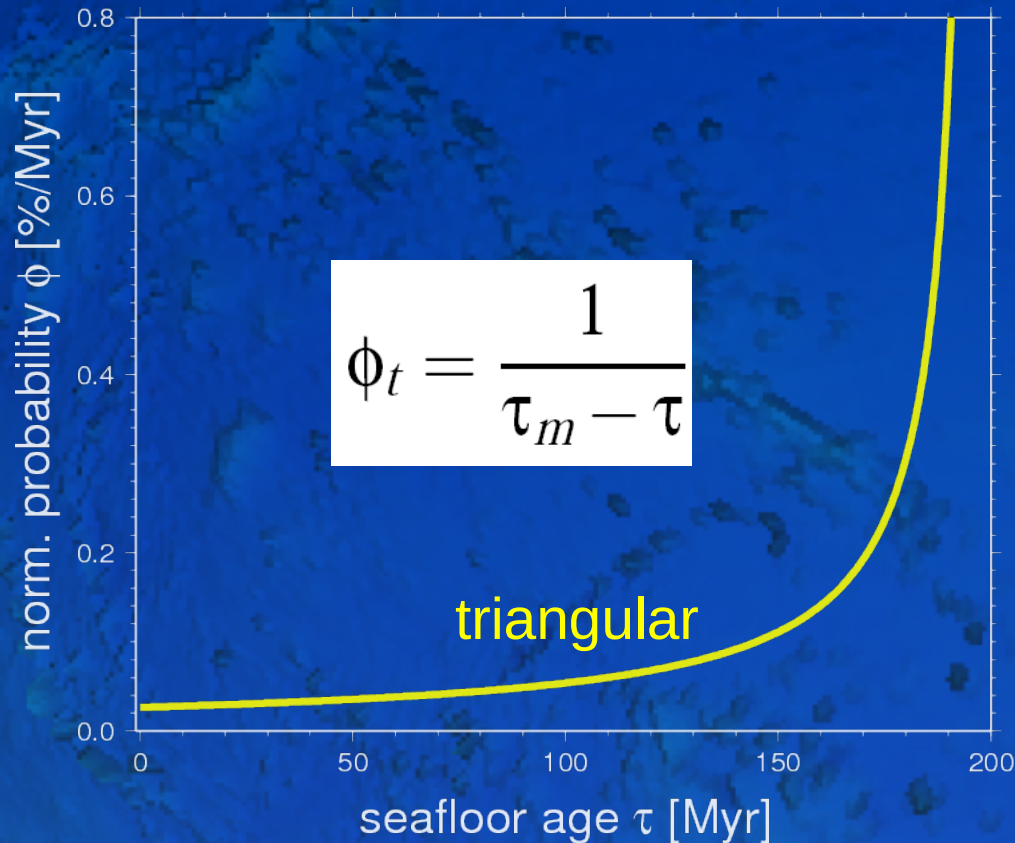
$$\Phi = c$$

$$\alpha(\tau, t = 0) \approx C_0(1 - \tau/\tau_m)$$

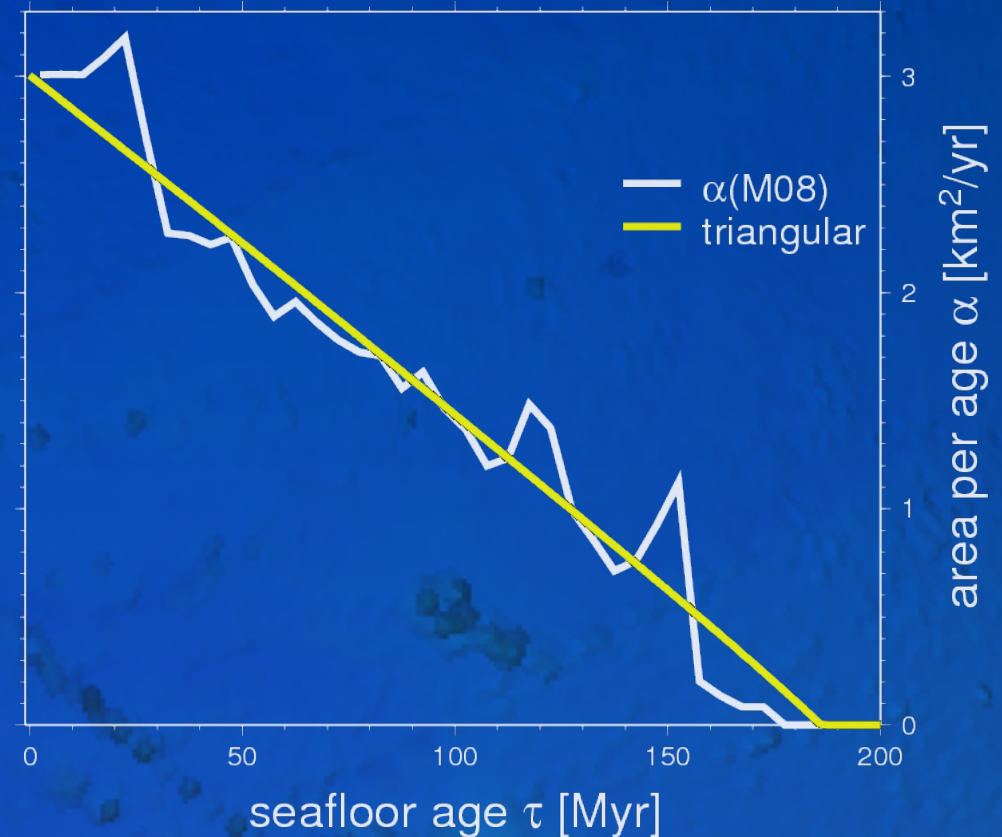


Alternative age distributions for constant production rates I

Subduction probability

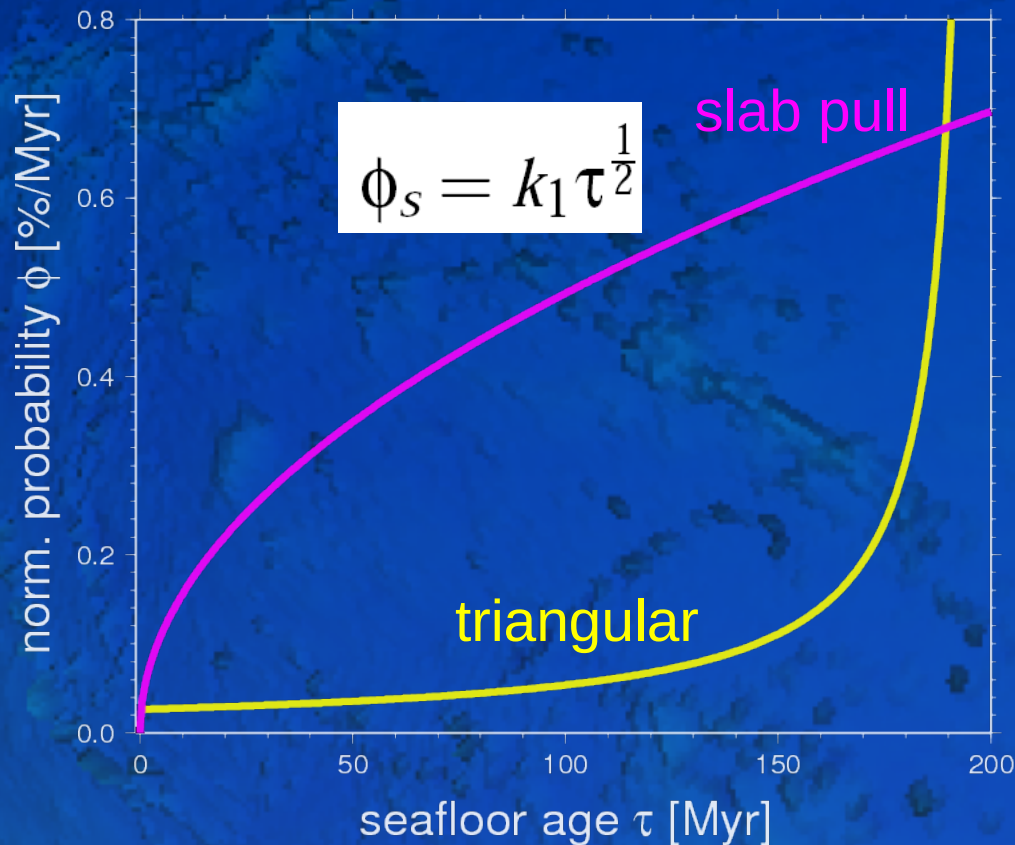


Age distribution

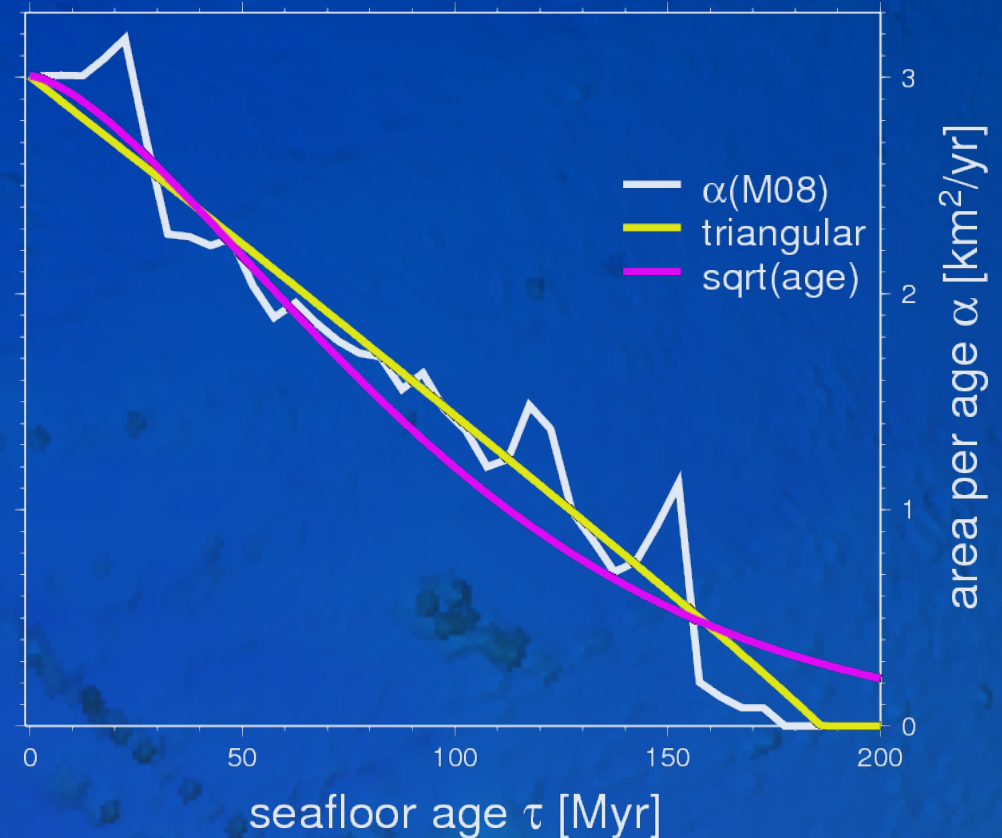


Alternative age distributions for constant production rates II

Subduction probability

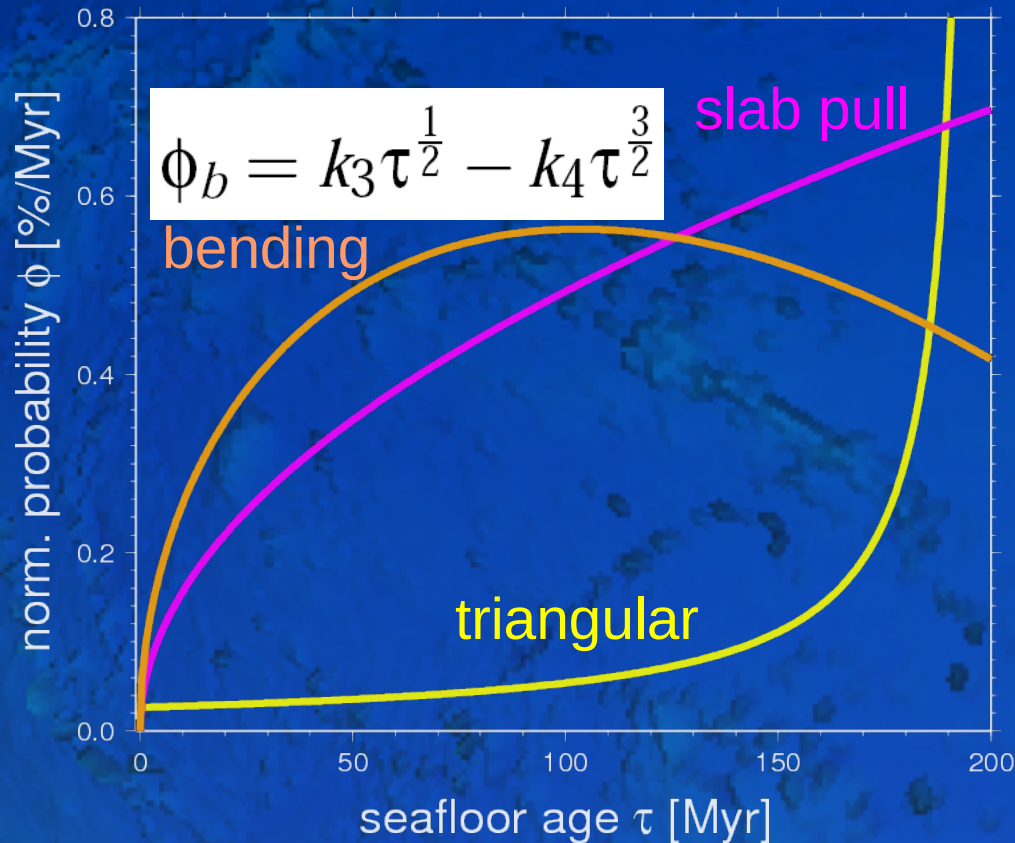


Age distribution

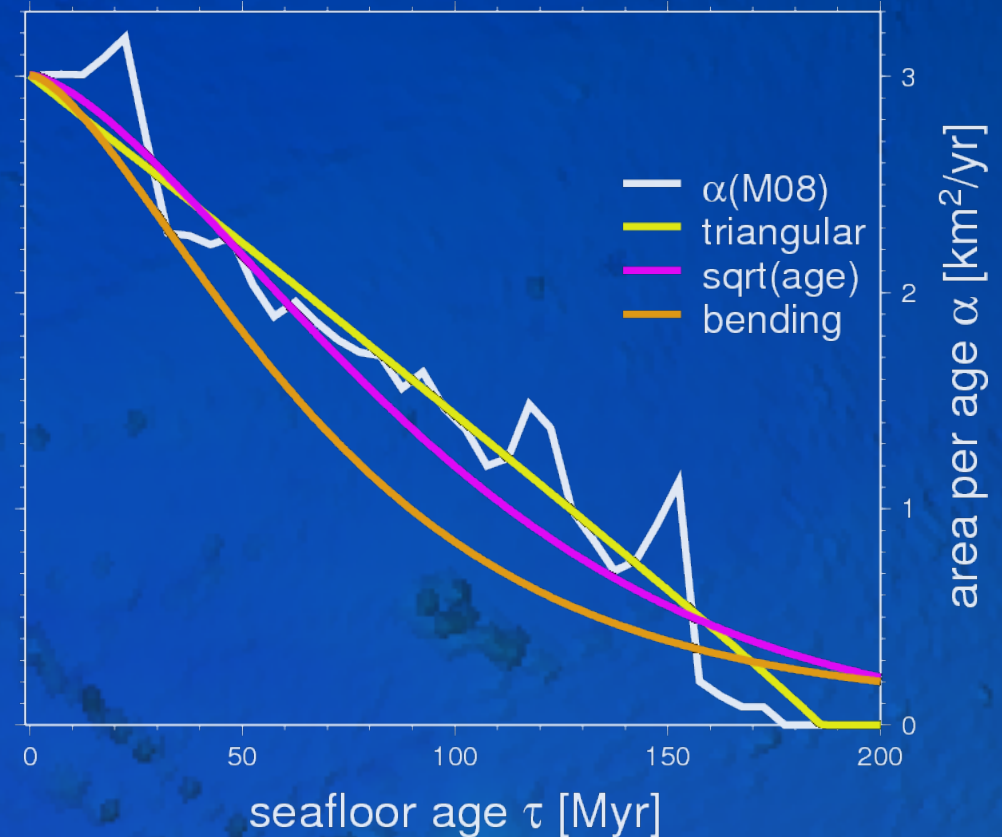


Alternative age distributions for constant production rates III

Subduction probability

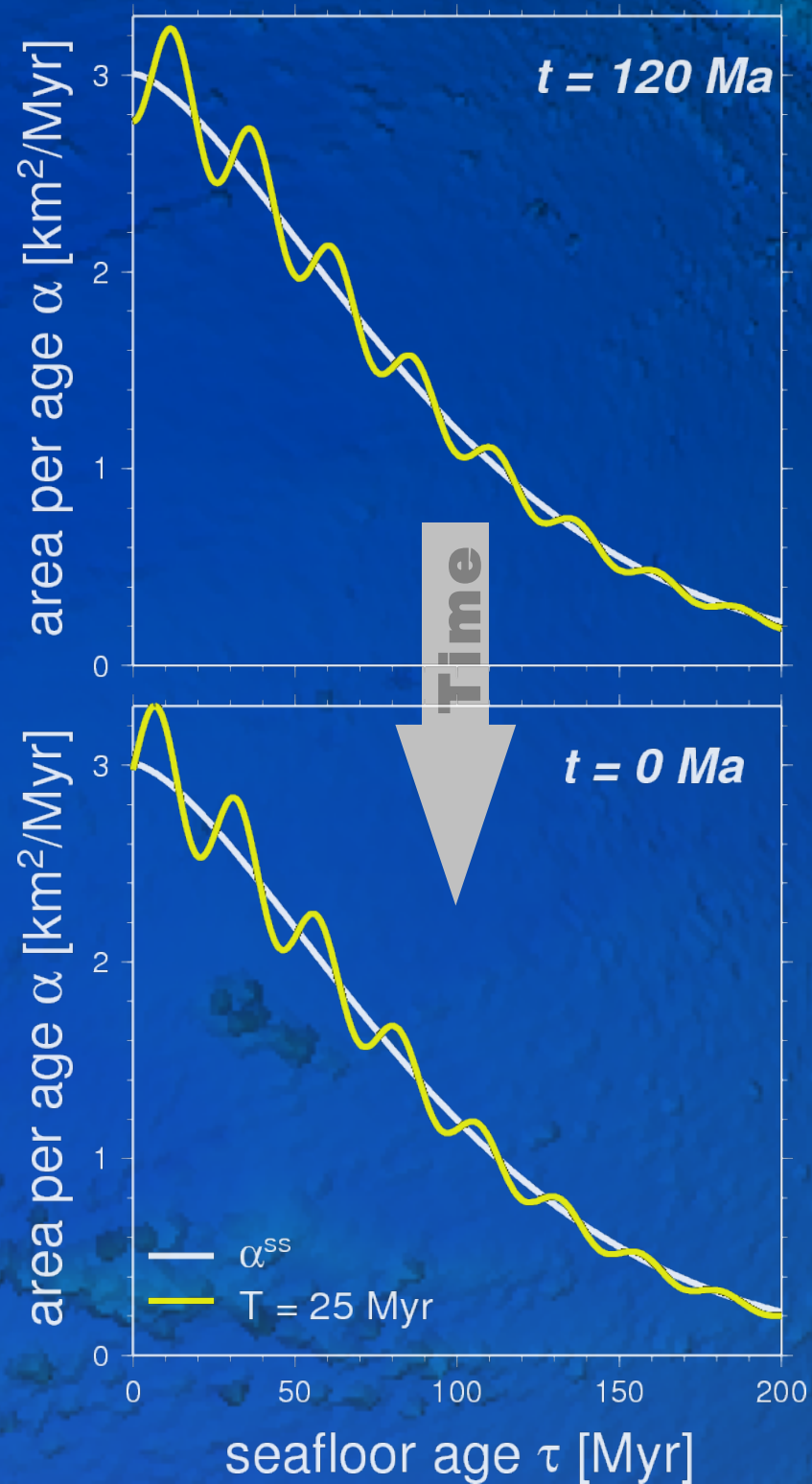


Age distribution



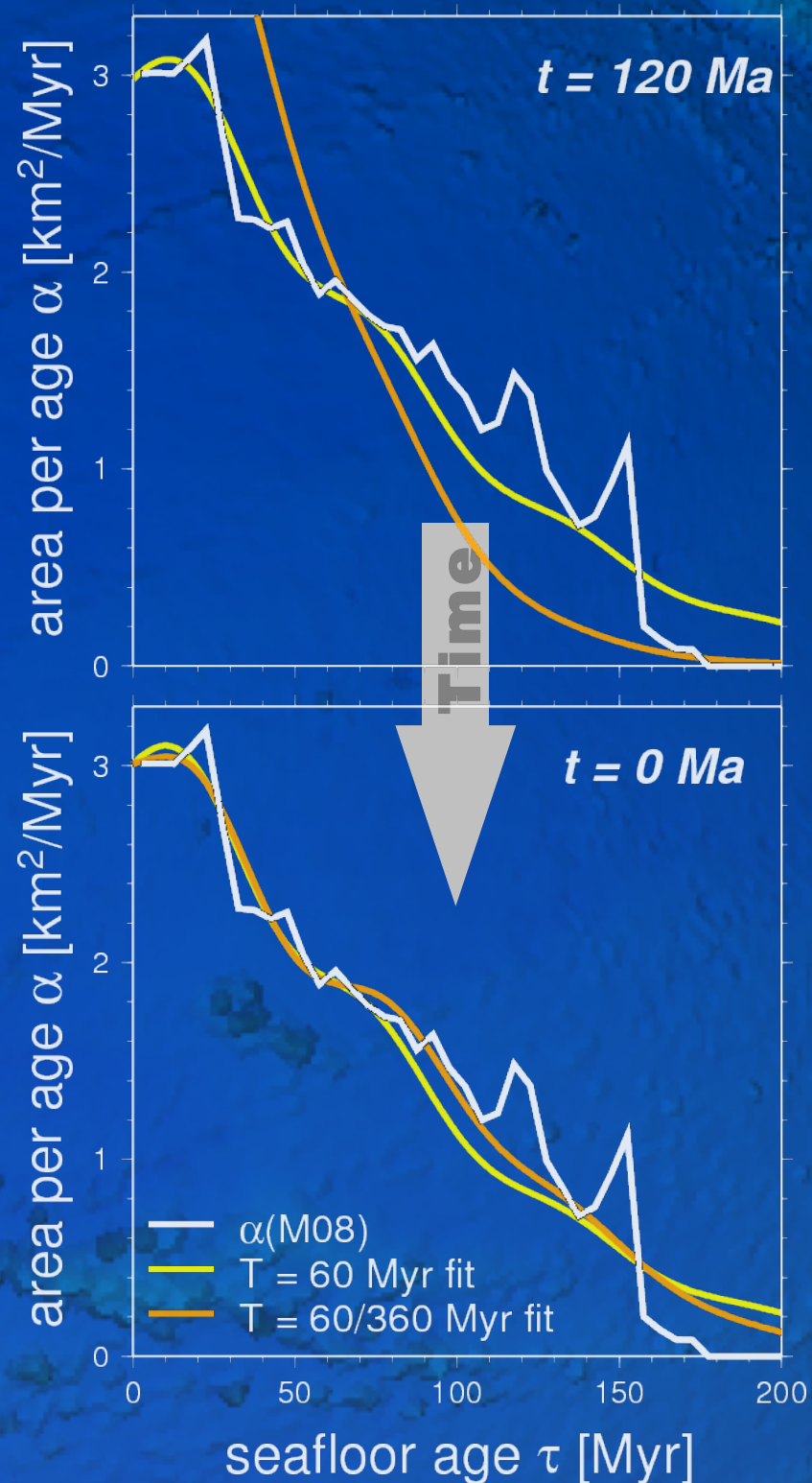
Time-variable seafloor production – Synthetic example

- Slab-pull ($\sqrt{\text{age}}$) probability
- Production rate variable at 10% amplitude with 25 Myr period

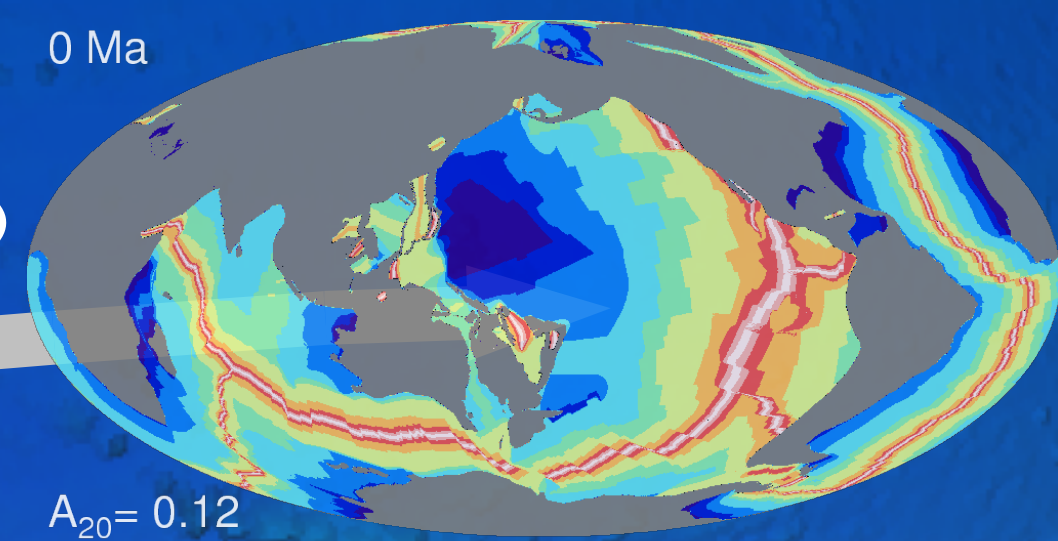
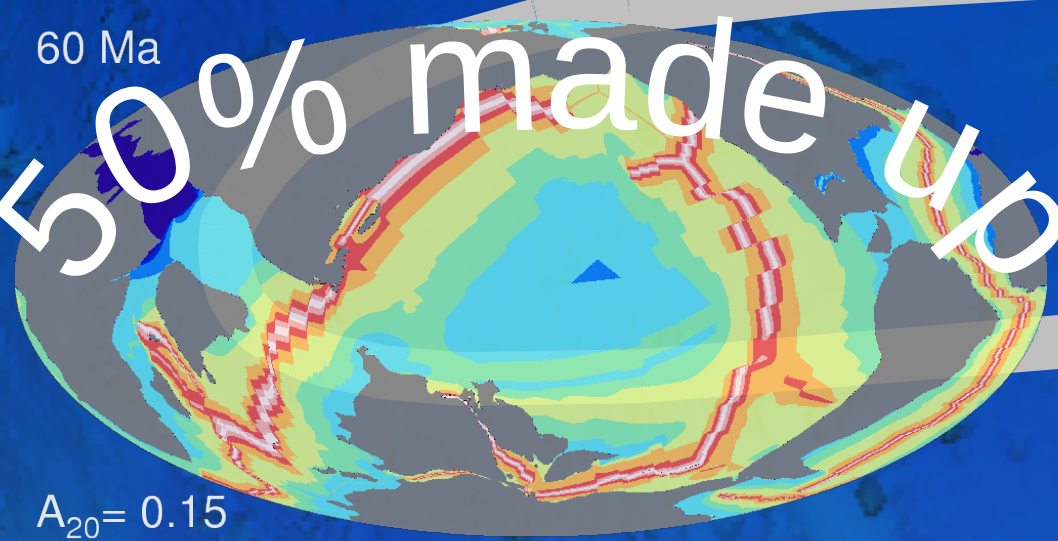
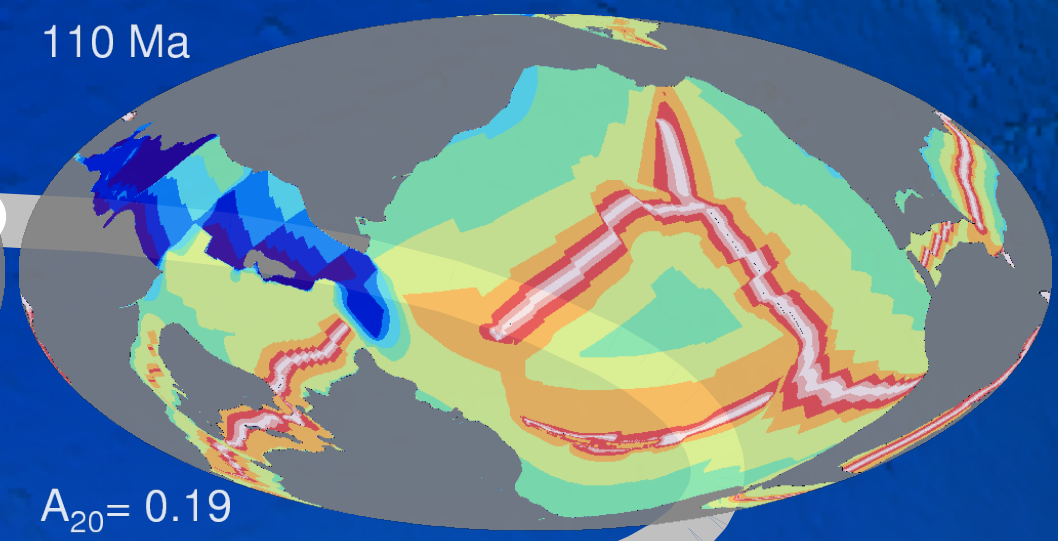
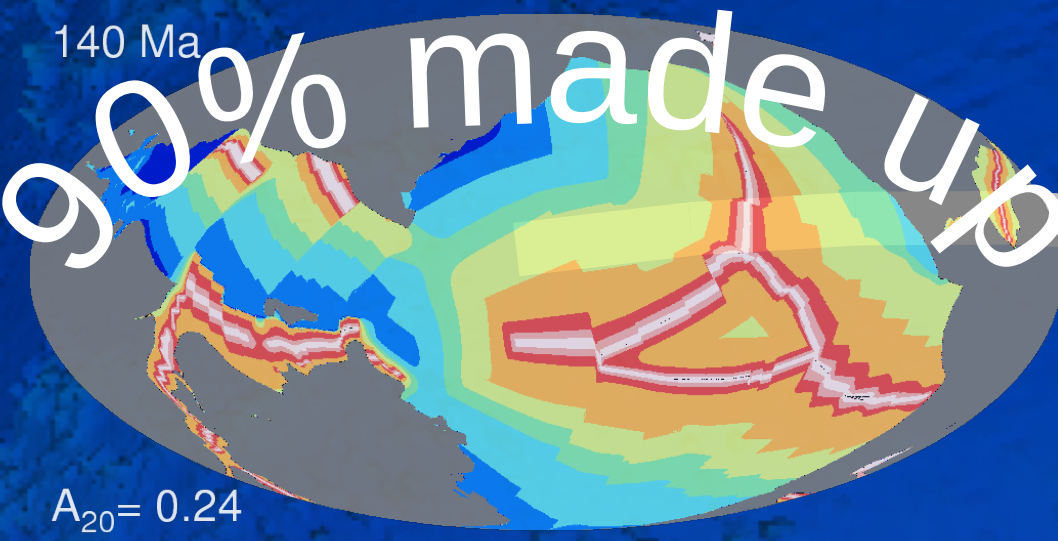


Time-variable production – Best-fit variability for present day age

- Single harmonic production variation at 6% amplitude and 60 Myr period
- Misfit $\chi^2 = 3$ compared to $\chi^2 = 4.8$ for steady triangular
- For two harmonics: $\chi^2 = 1.9$
- Broad trends are captured by 1-D model, details will depend on ridge jumps, continents etc.

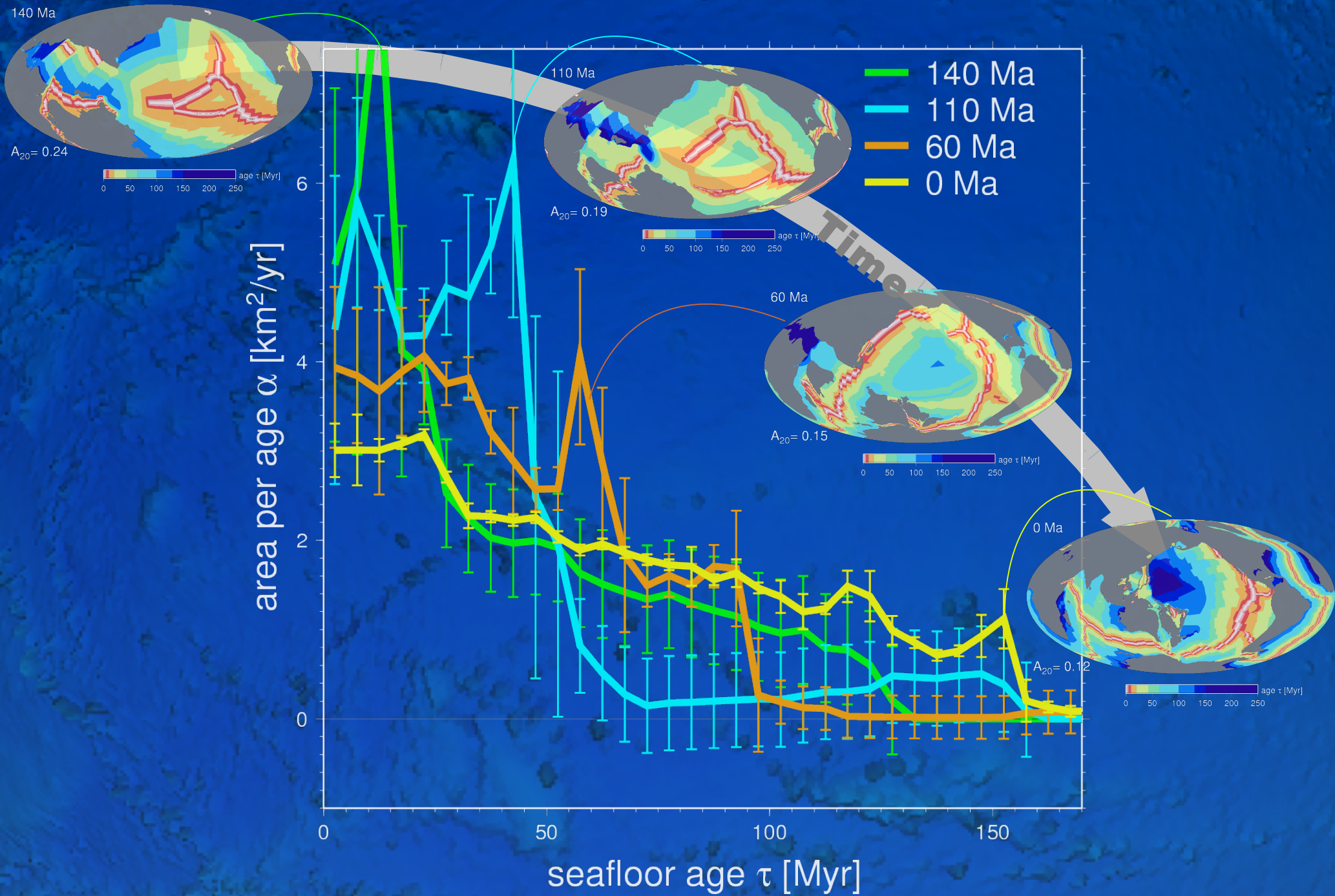


Seafloor age reconstructions

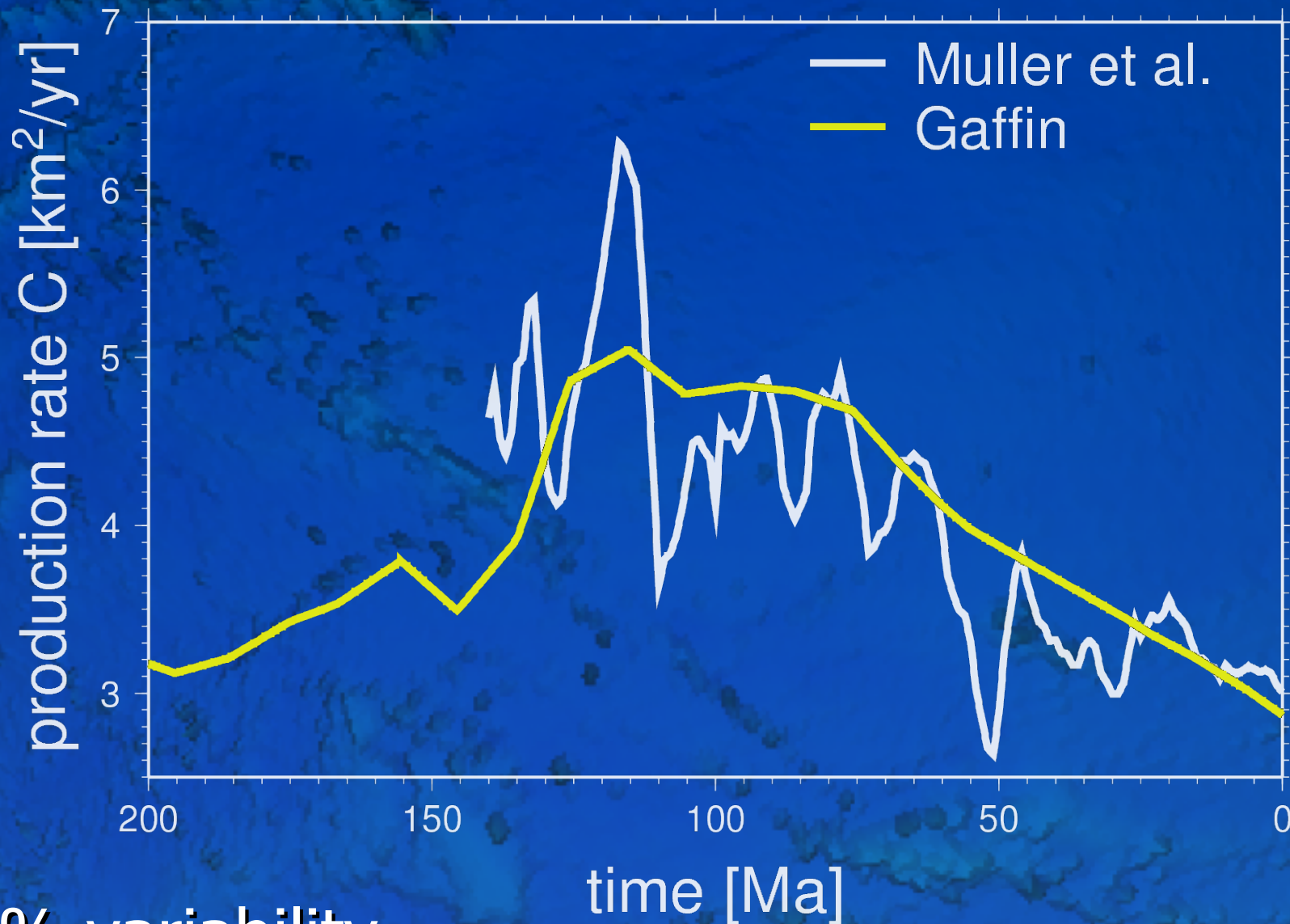


Time ←

Reconstructed age distributions

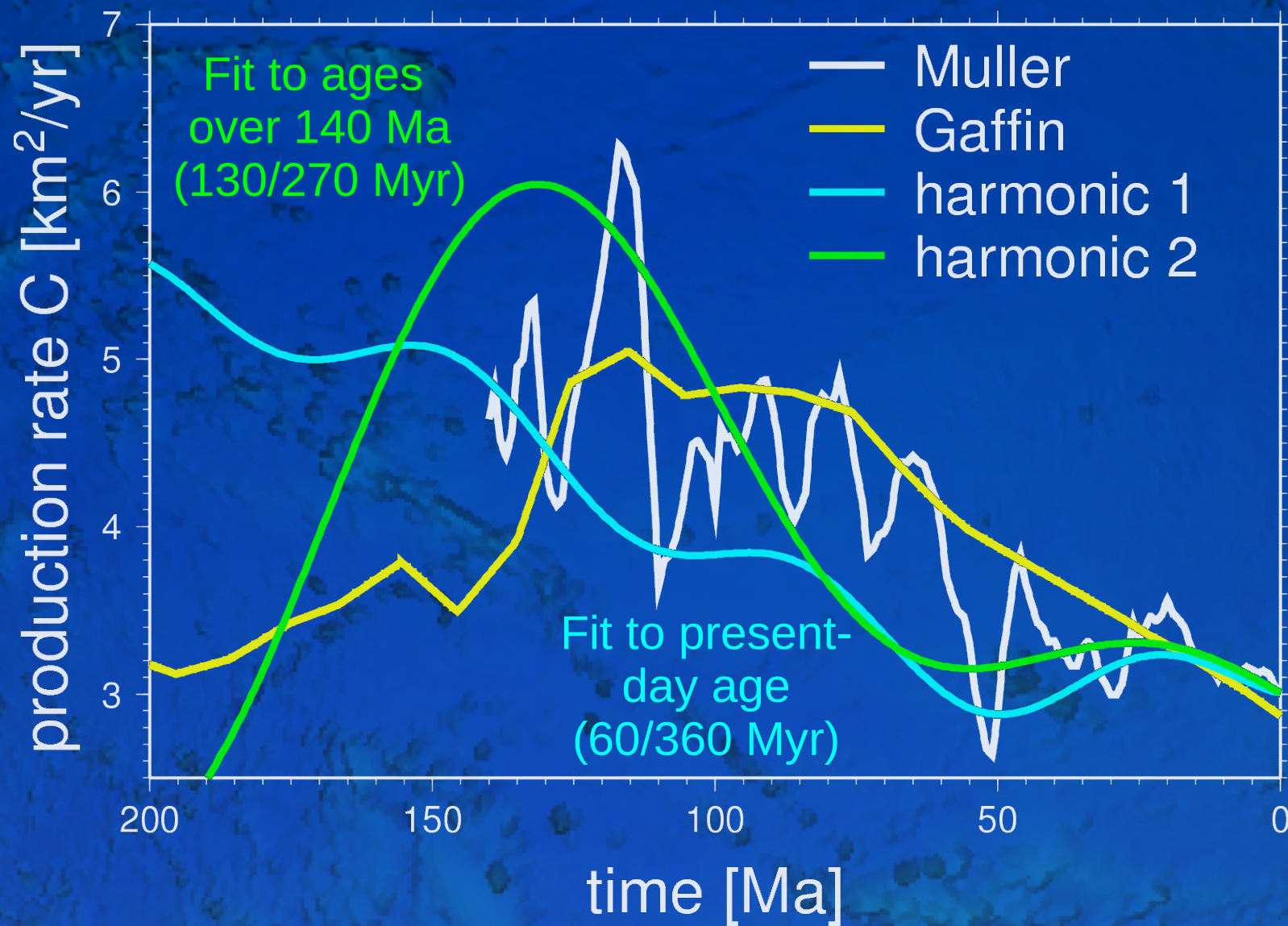


Geologically inferred seafloor production rate variations



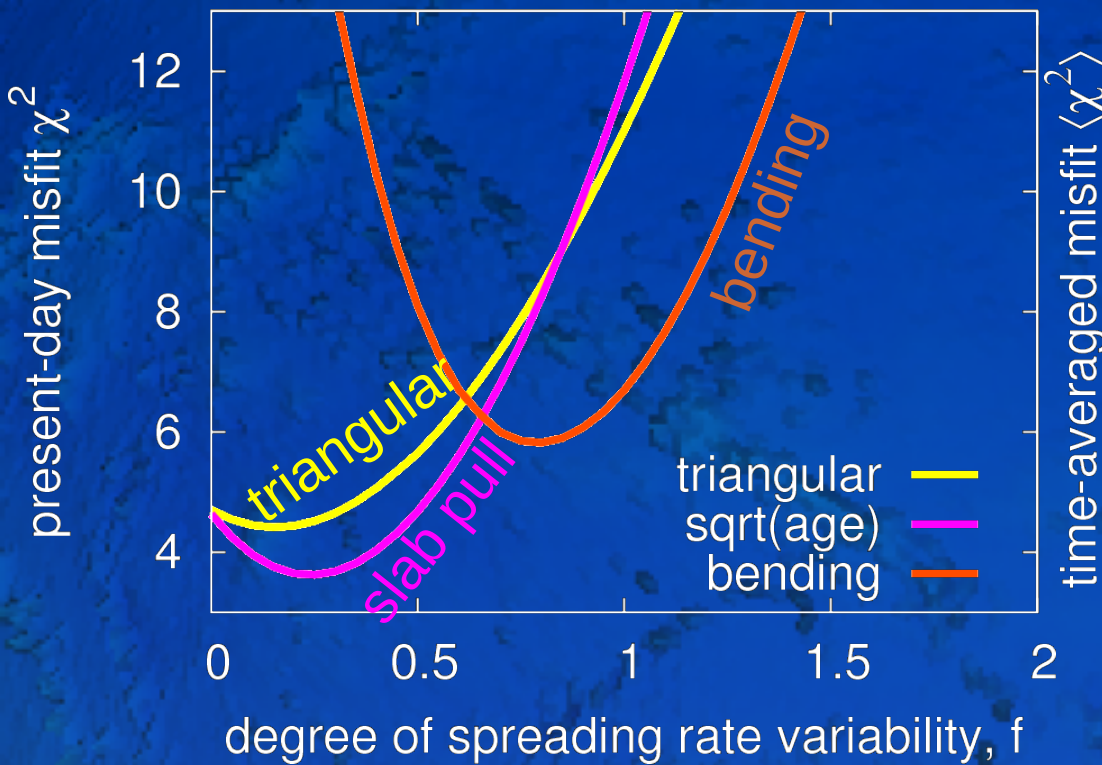
- **~20% variability**

Best-fit spreading rate variations



Age misfit as a function of geologically inferred spreading variability

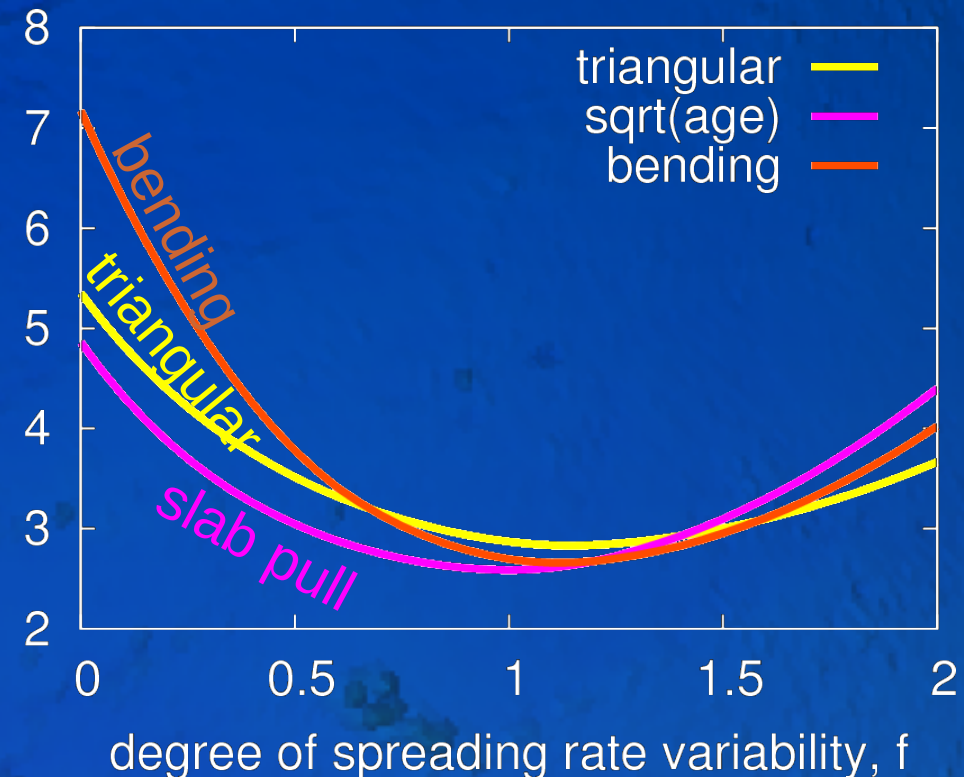
Misfit to present-day



Constant production

Two times geological

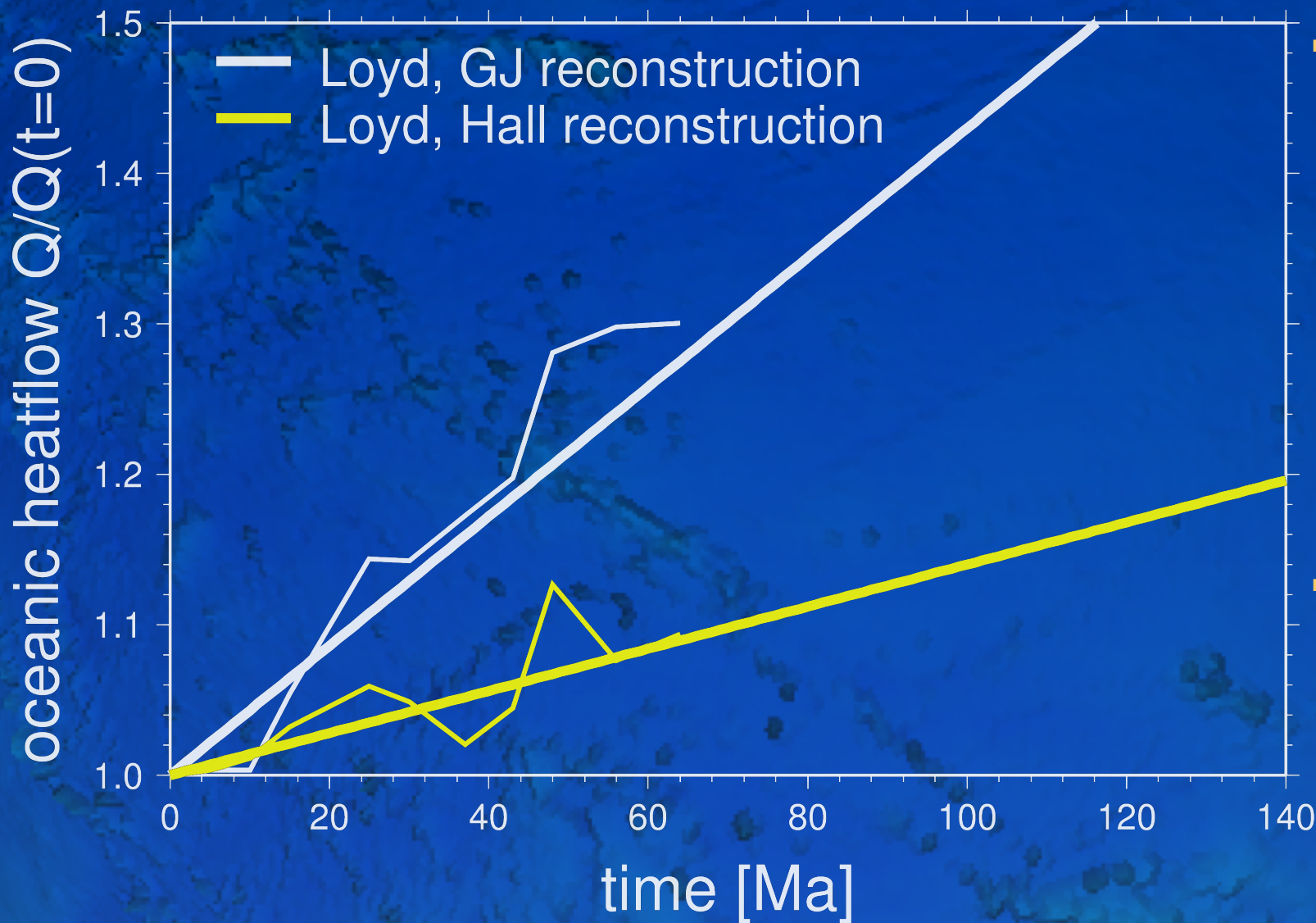
Misfit over 140 Ma



Constant production

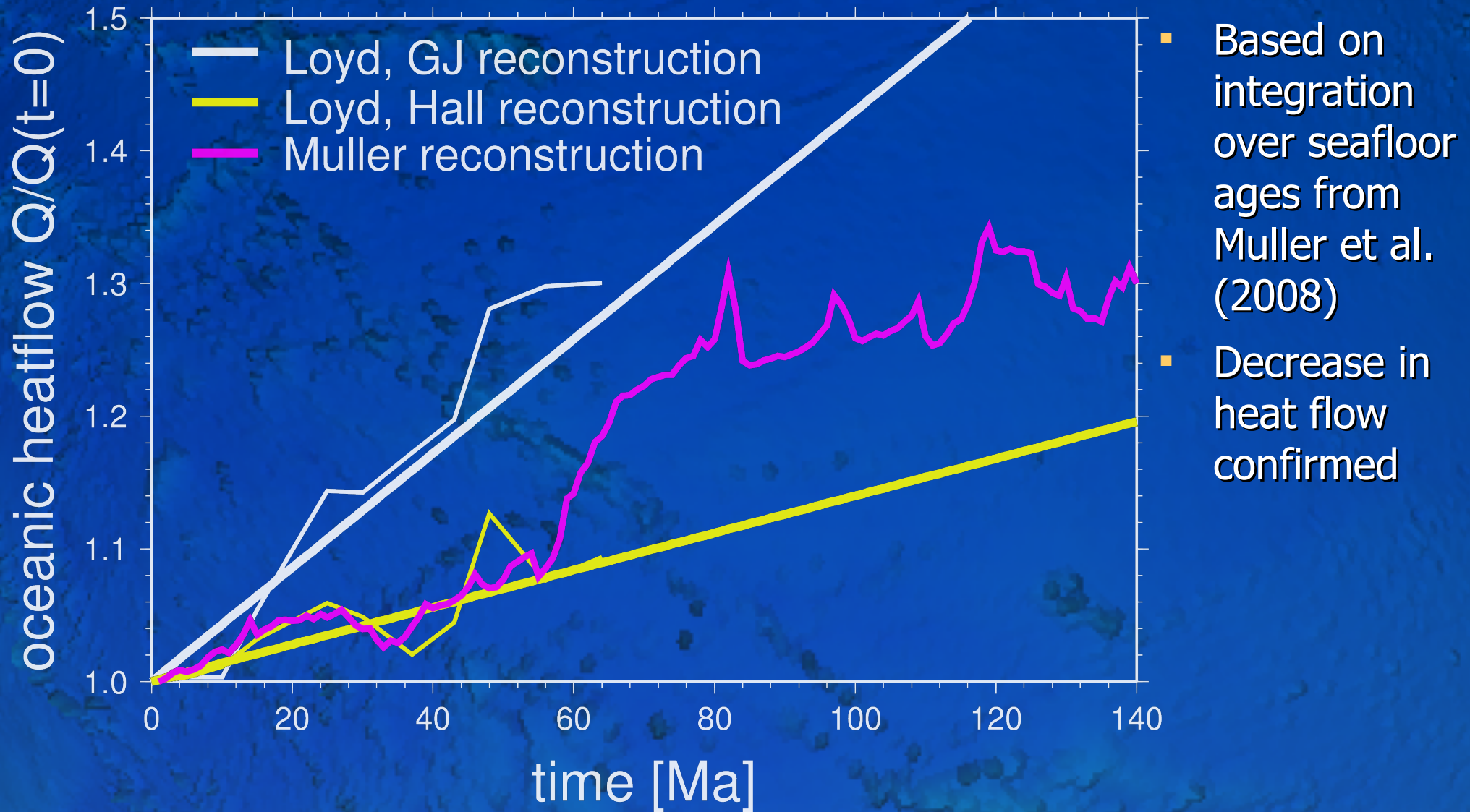
Two times geological

Variations in heat flow over 60 Ma

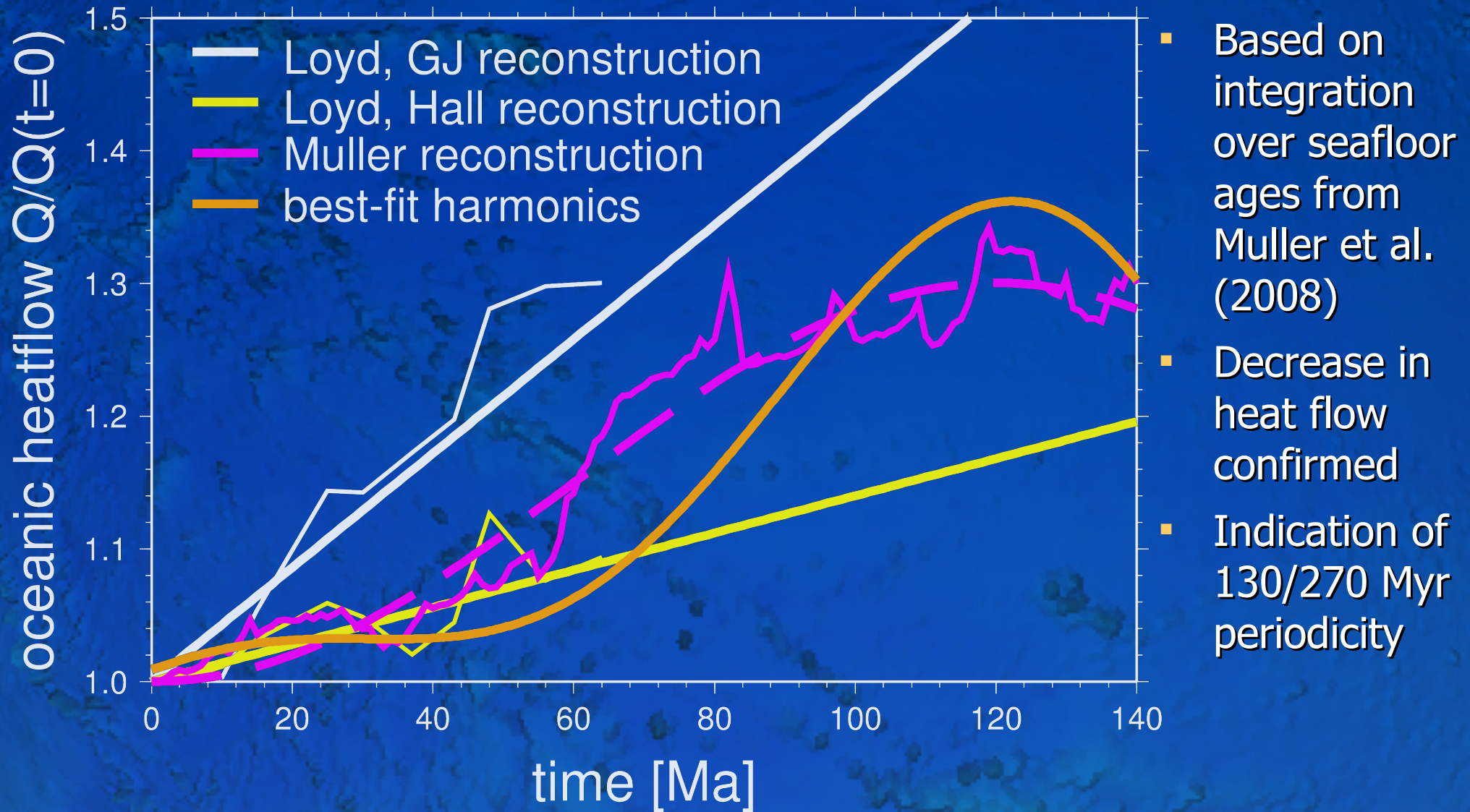


- Based on integration over seafloor ages from Xu et al. (2006) using a modified half-space cooling law
- Significant decrease in heat flow and relative sealevel

Variations in heat flow over 120 Ma



Variations in heat flow over 120 Ma



Conclusions from seafloor age modeling

- Slab-pull subduction probability and variable seafloor production rate work as well as, or better than, the triangular, constant scenario (cf. Demicco, 2004)
- Slab-pull plus bending might provide good parametrization of oceanic plate system
- Heat flow has decreased by $\sim 0.25\%/Ma$ over Cenozoic (cf. Harrison, 1980; Loyd et al., 2007)
- Indication of ~ 60 Myr and ~ 270 Myr periodicity in seafloor production
- Plate tectonics is not about to shut down

Context for heat flow variations:

Parameterized convection models

- Can use volume and time-averaged equation for mantle temperature T to gain some insight

- Ingredients:

- Assumptions about radiogenic heating, Urey ratio $\gamma(0)$ for present day

- Scaling relationship between Rayleigh number ($f(T, \text{viscosity } \eta)$) and heat flux

- Assumes traditionally that boundary layer analysis for isochemical convective system holds, $\beta \sim 1/3$

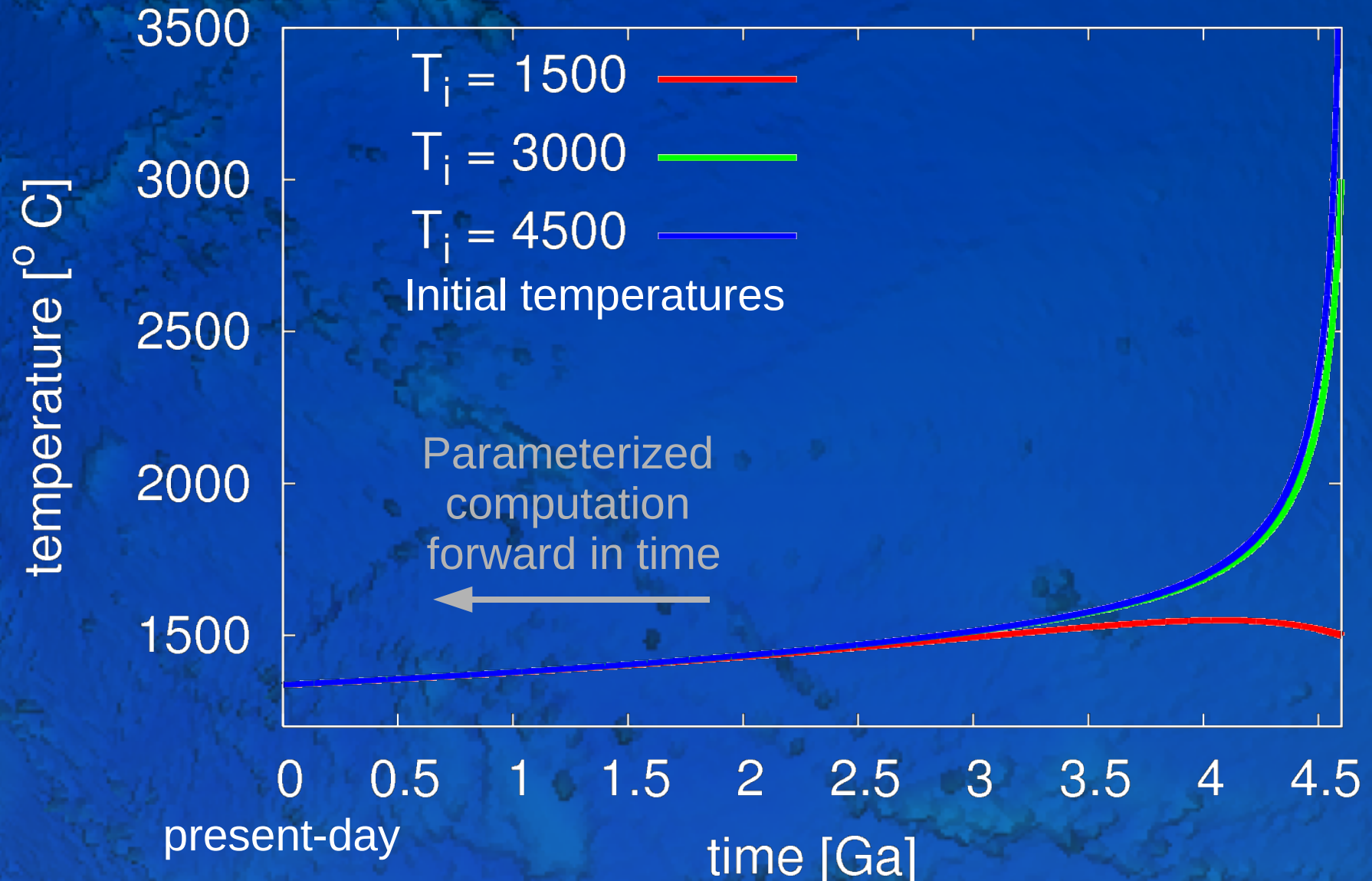
$$Q_{convec} \propto Ra(T, \eta)^\beta$$

or

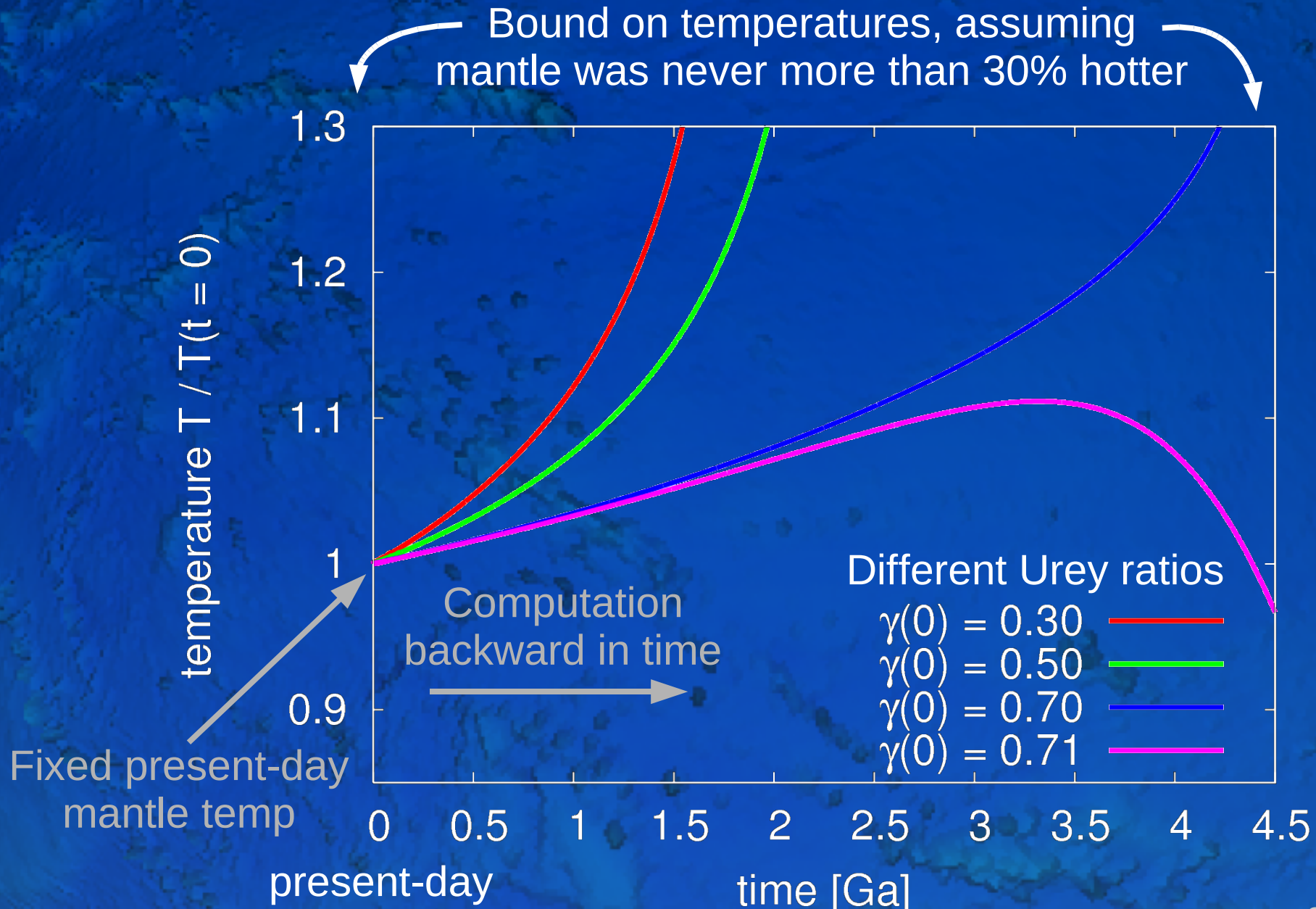
$$Q \propto \frac{T_i^{\beta+1}}{\eta (T_i)^\beta}$$

The Tozer (1972) thermostat

Heat flow scaling $\beta = 1/3$, $\gamma = 0.6$ Urey ratio

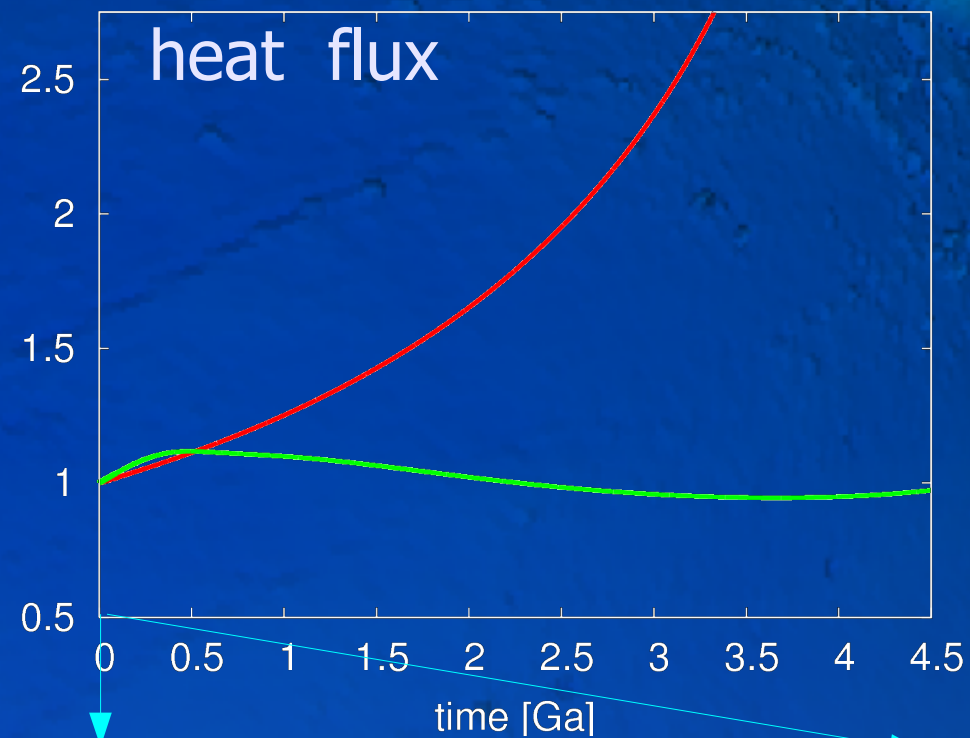
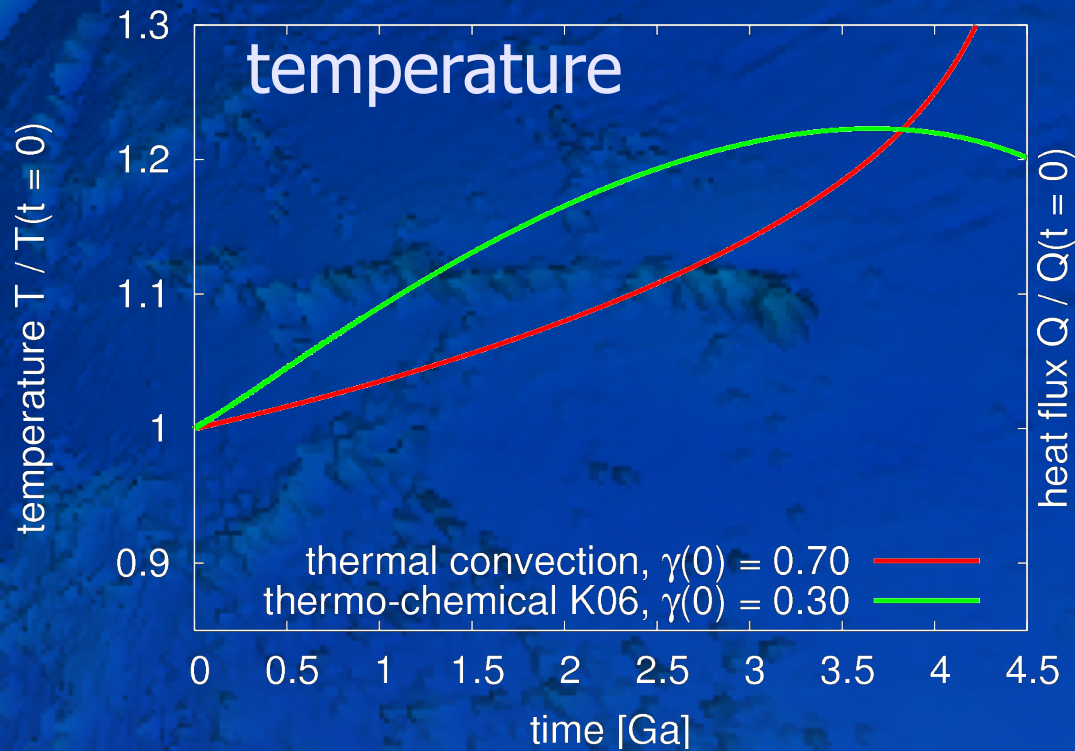


The thermal catastrophe for $\beta = 1/3$

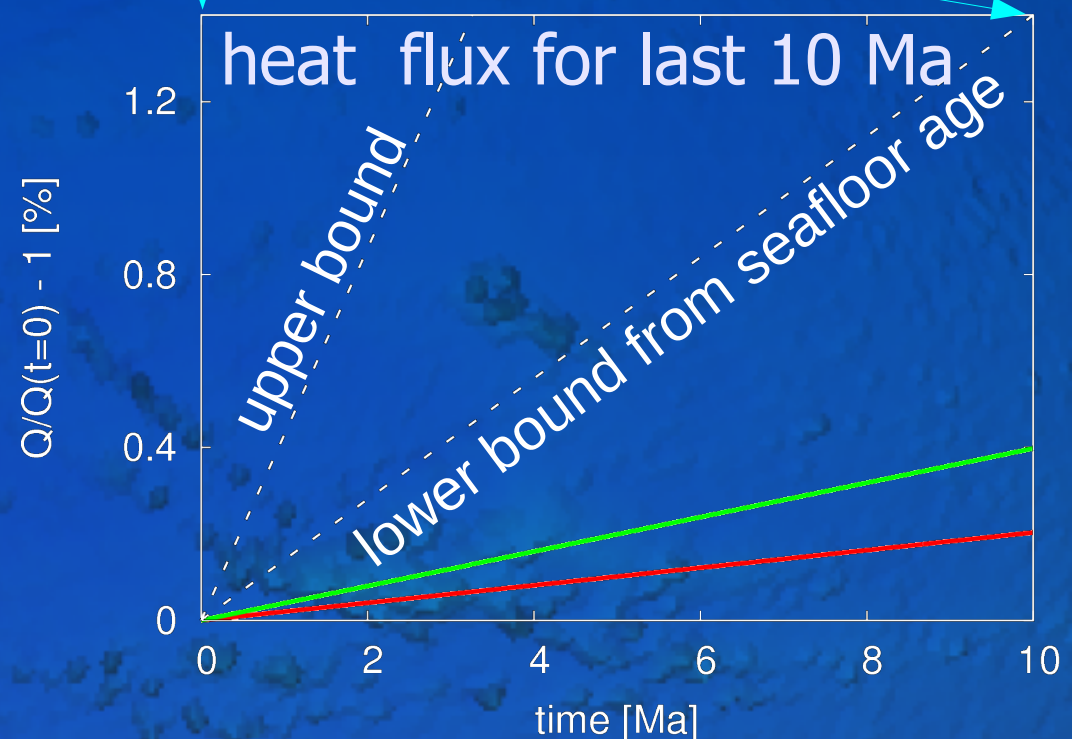


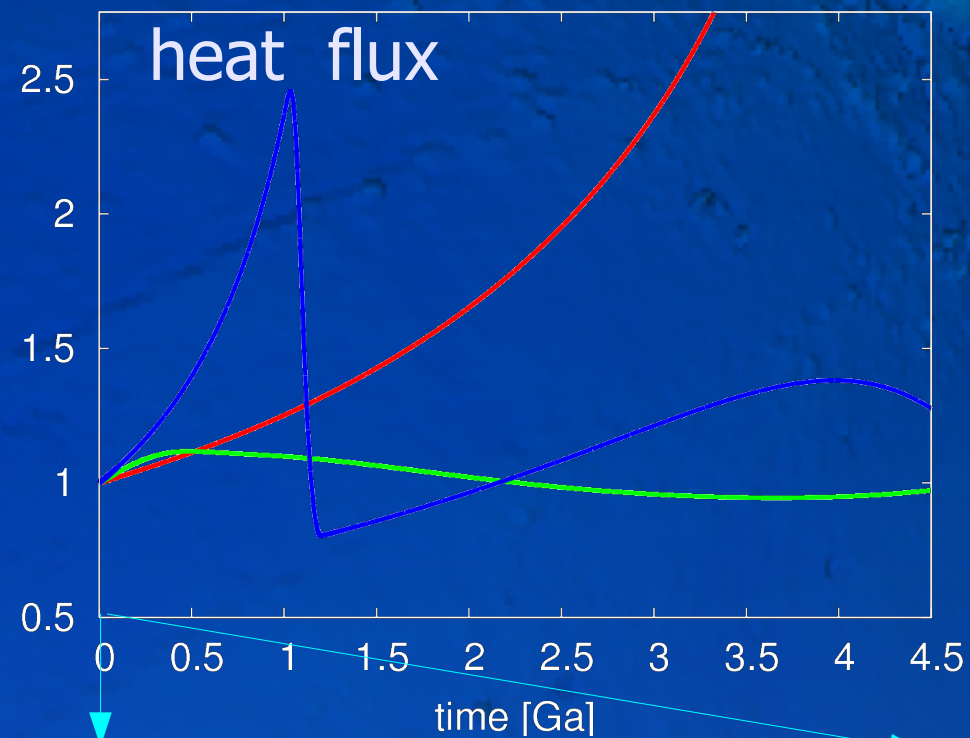
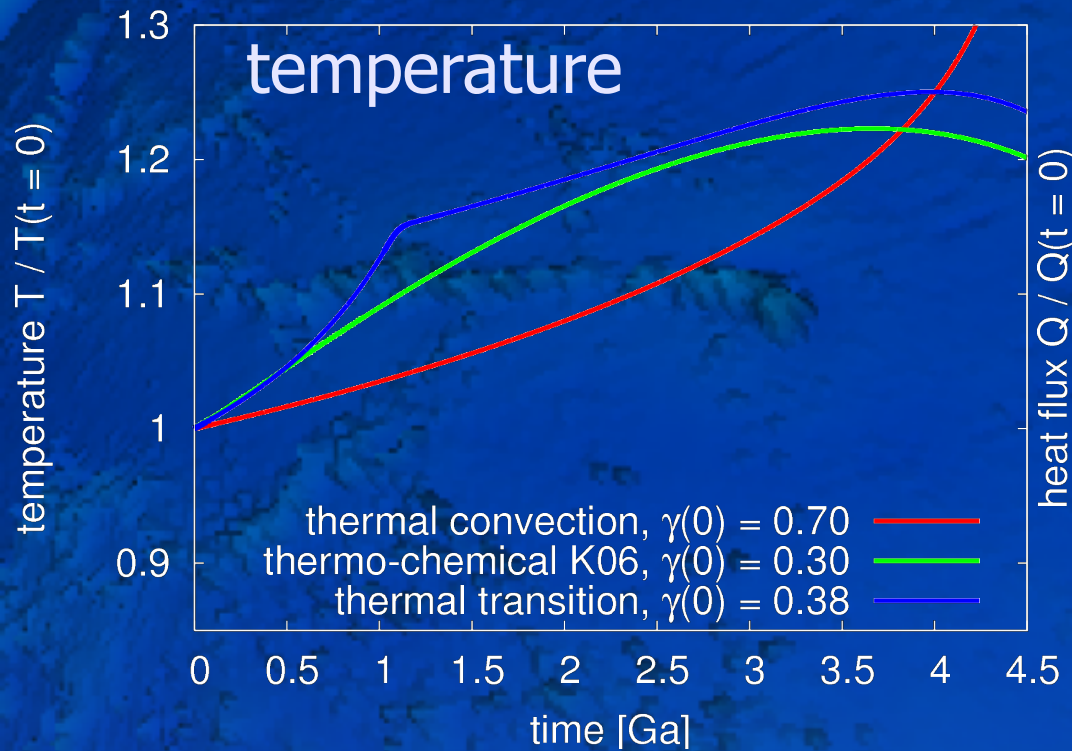
Chemical boundary layers and bending

- Viscous dissipation in slab bending of importance for plate velocities (Conrad & Hager, 1999a; Becker et al., 1999; Buffett, 2006)
 - $\beta \downarrow$ (Conrad & Hager, 1999b)
- Fractionation (melting column $f(T)$) at ridges affects density and viscosity (via volatiles) (i.e. thermo-chemical boundary layers, e.g. Lee et al., 2005)
 - $\beta \downarrow\downarrow$ (Korenaga, 2003)

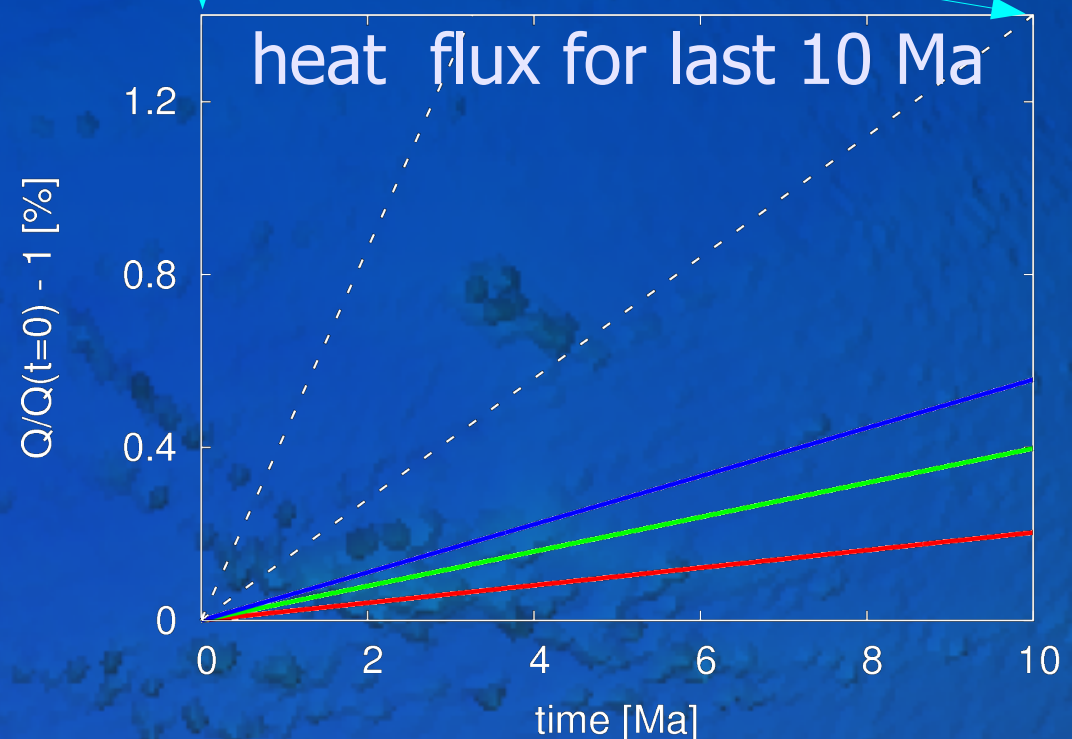


- Unpleasantly aside, the thermo-chemical scaling keeps the mantle chill for Urey ~ 0.3
- Neither model leads to large heat flux rate change over last 500 Ma



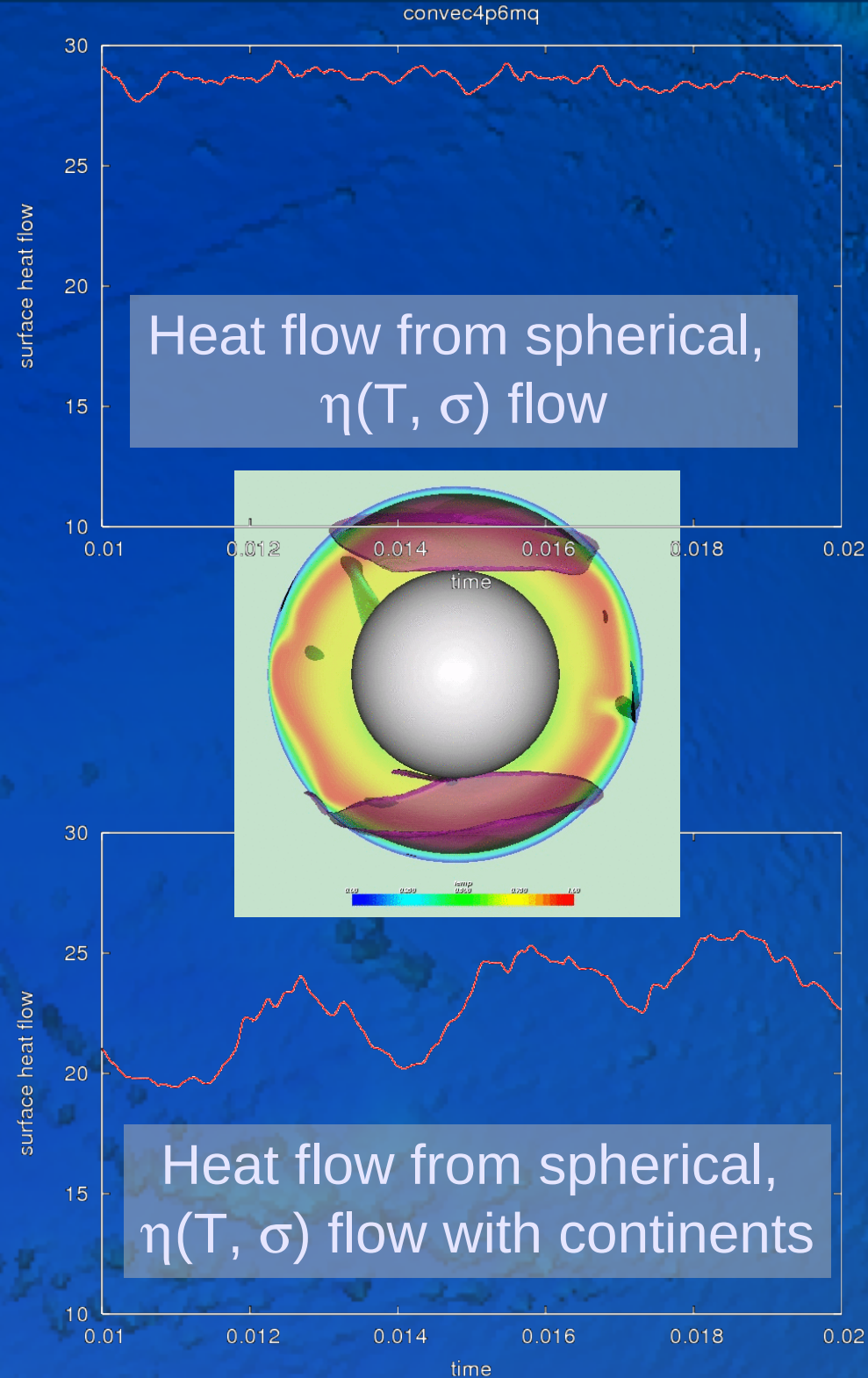


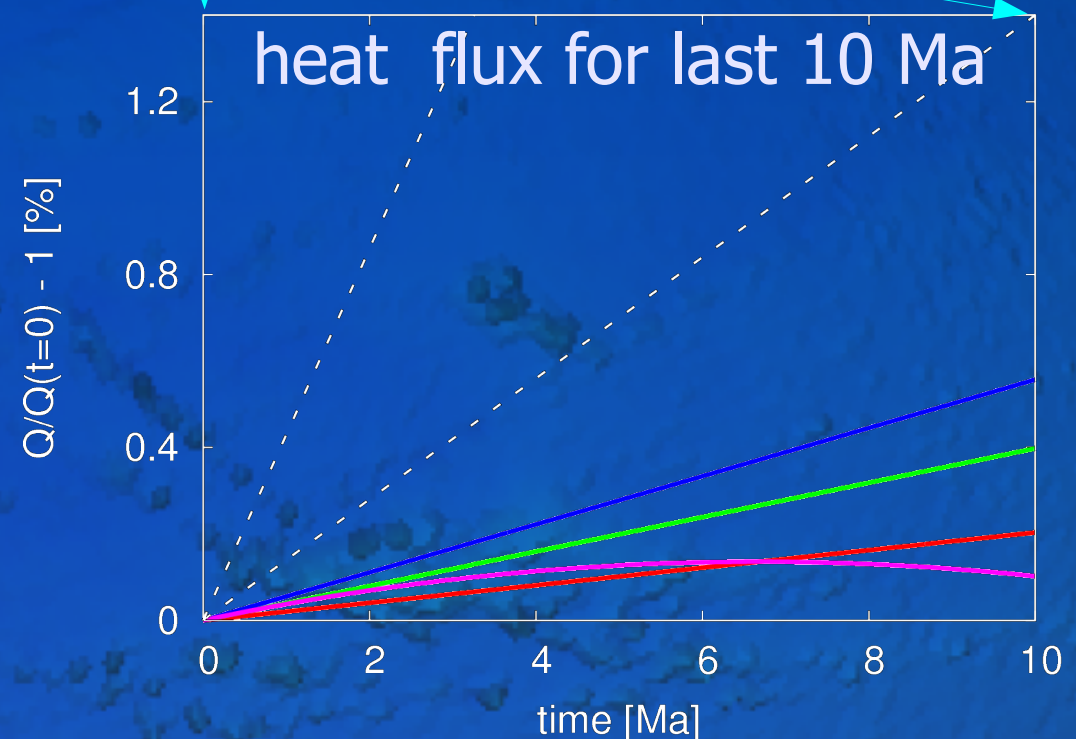
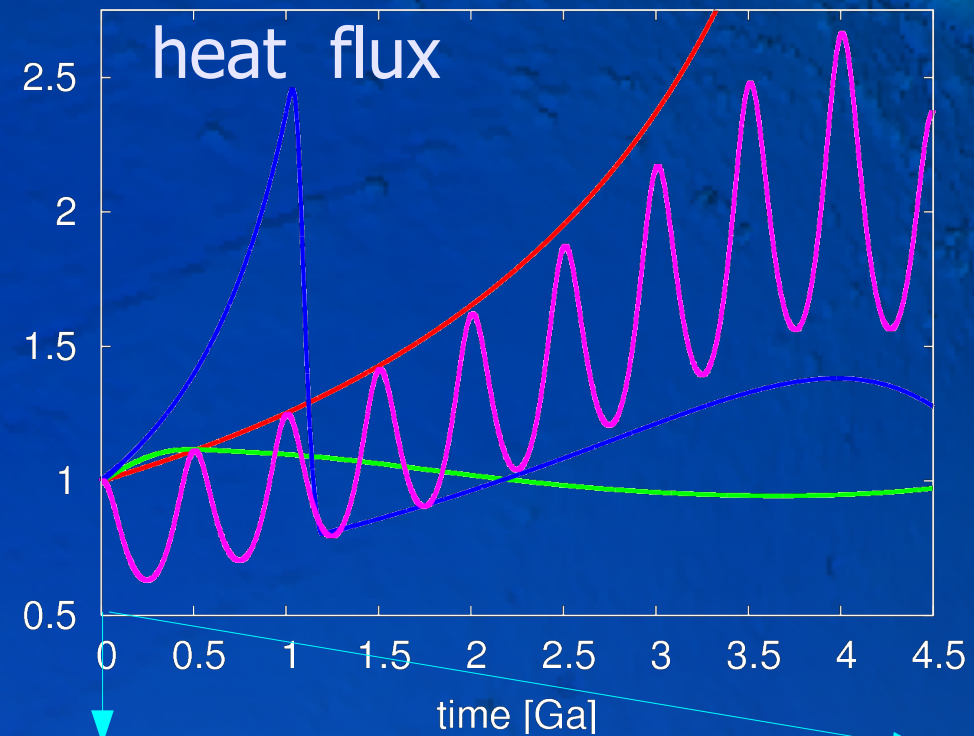
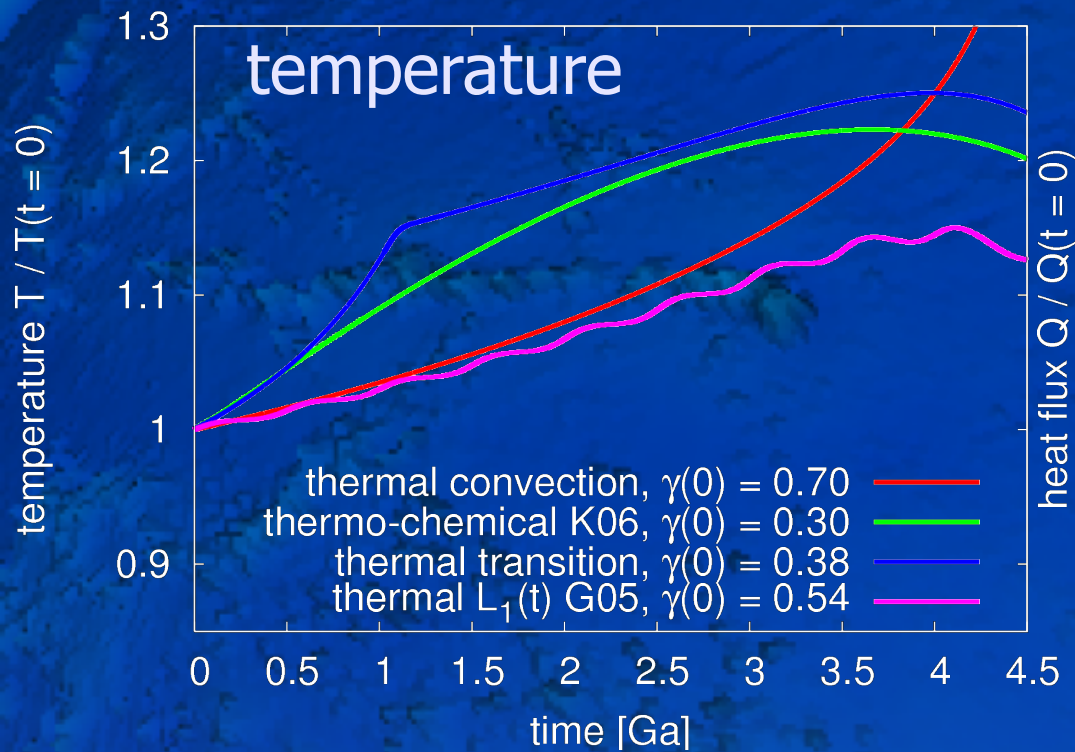
- Transition from inhibited heat flux at 1 Ga (e.g. rigid lid) does not lead to large rates of heat flux change for last 10 Ma, either



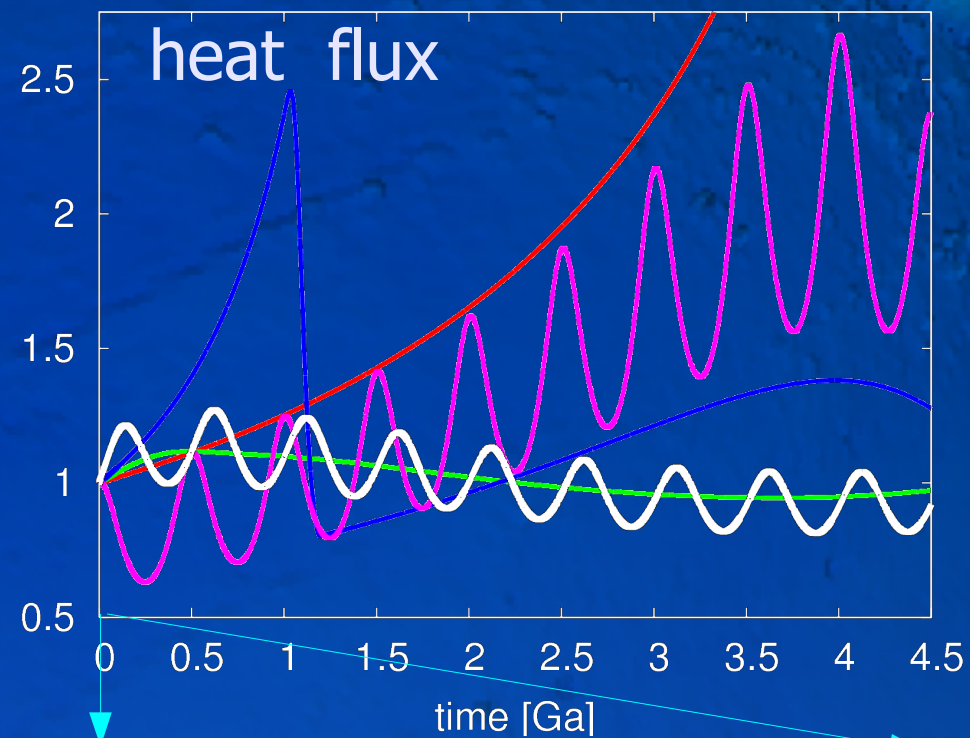
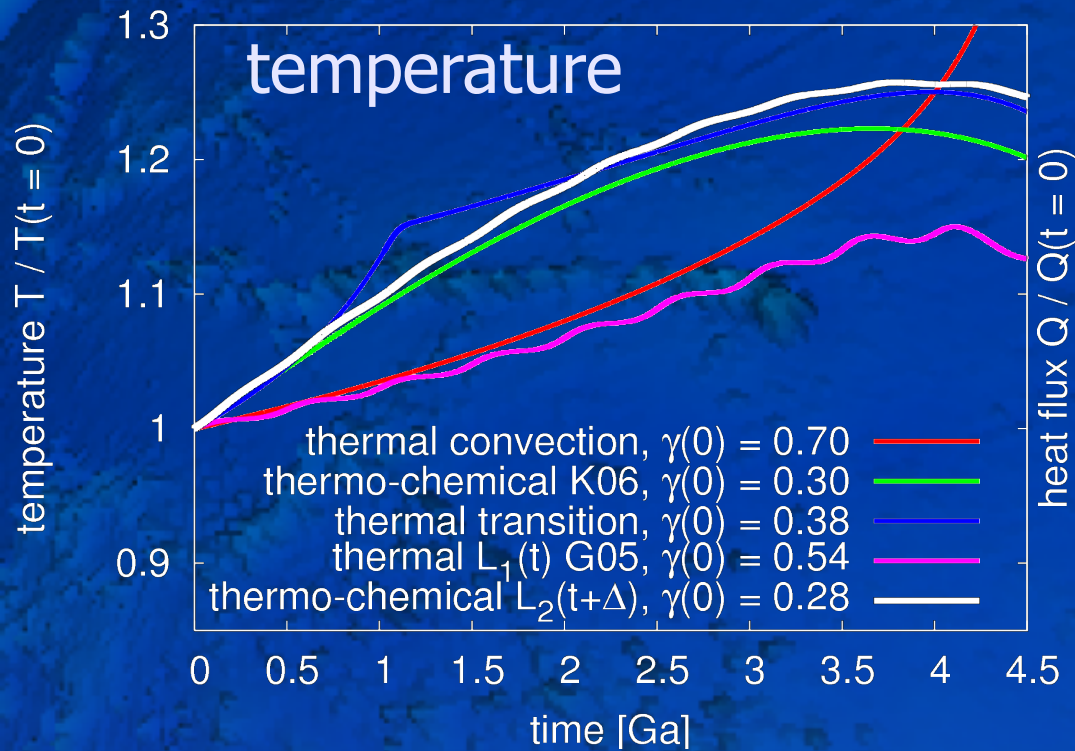
Episodic heat flow

- Fluctuations in heat flow are, of course, expected from geodynamical models
- +/- 0.1%/Ma for mobile lid (e.g. Moresi & Solomatov, 1999), more for dramatic reorganizations (e.g. Stein et al., 2004; Zhong et al., 2007)
- Dearth of "realistic" models with continents and viscoplastic rheology (not much longer)

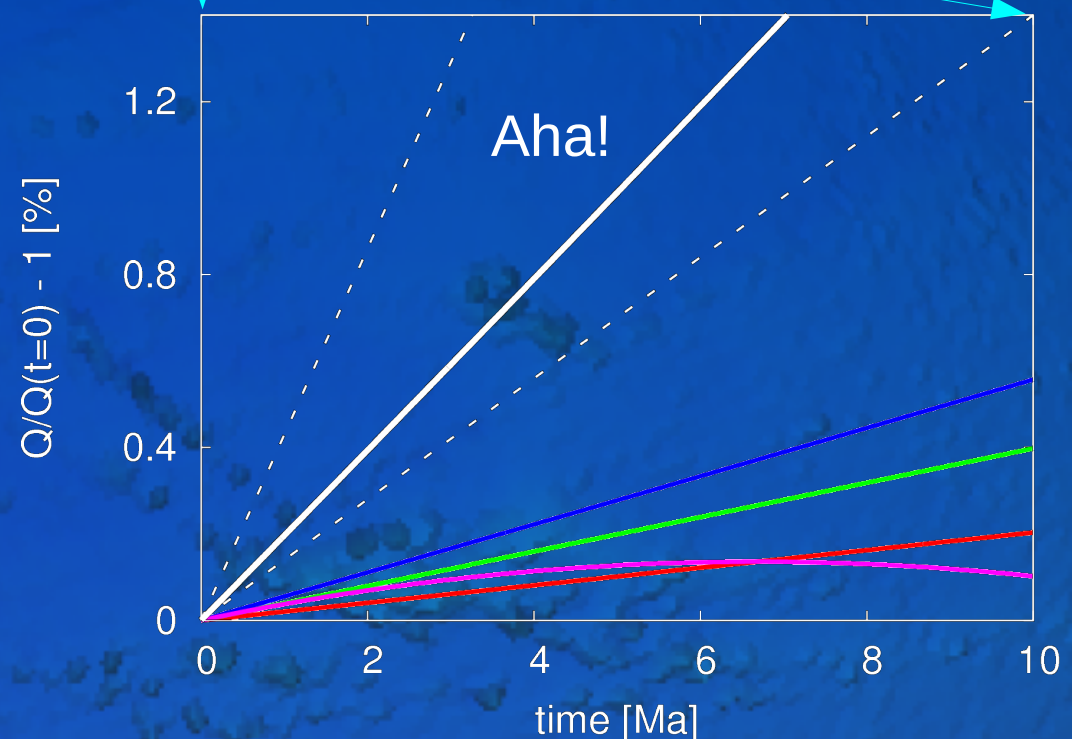




- Grigne et al. (2005) model gives large fluctuations in heat flux, but the phase is off compared to what we infer for the Cenozoic



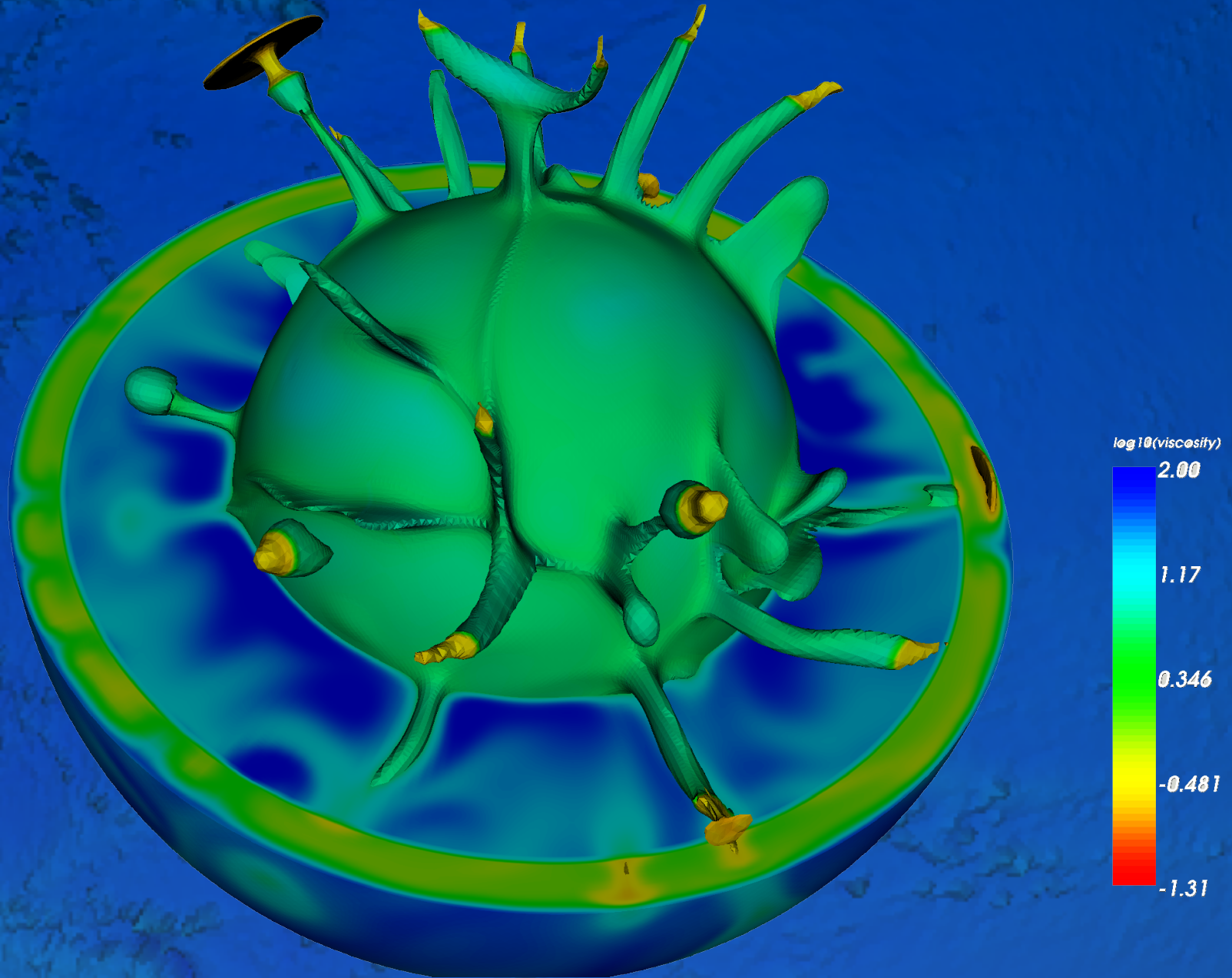
- A cyclic, thermo-chemical solution for changes in convective wavelength works for dQ/dt and $T(\text{Archean})$ for Urey ~ 0.3



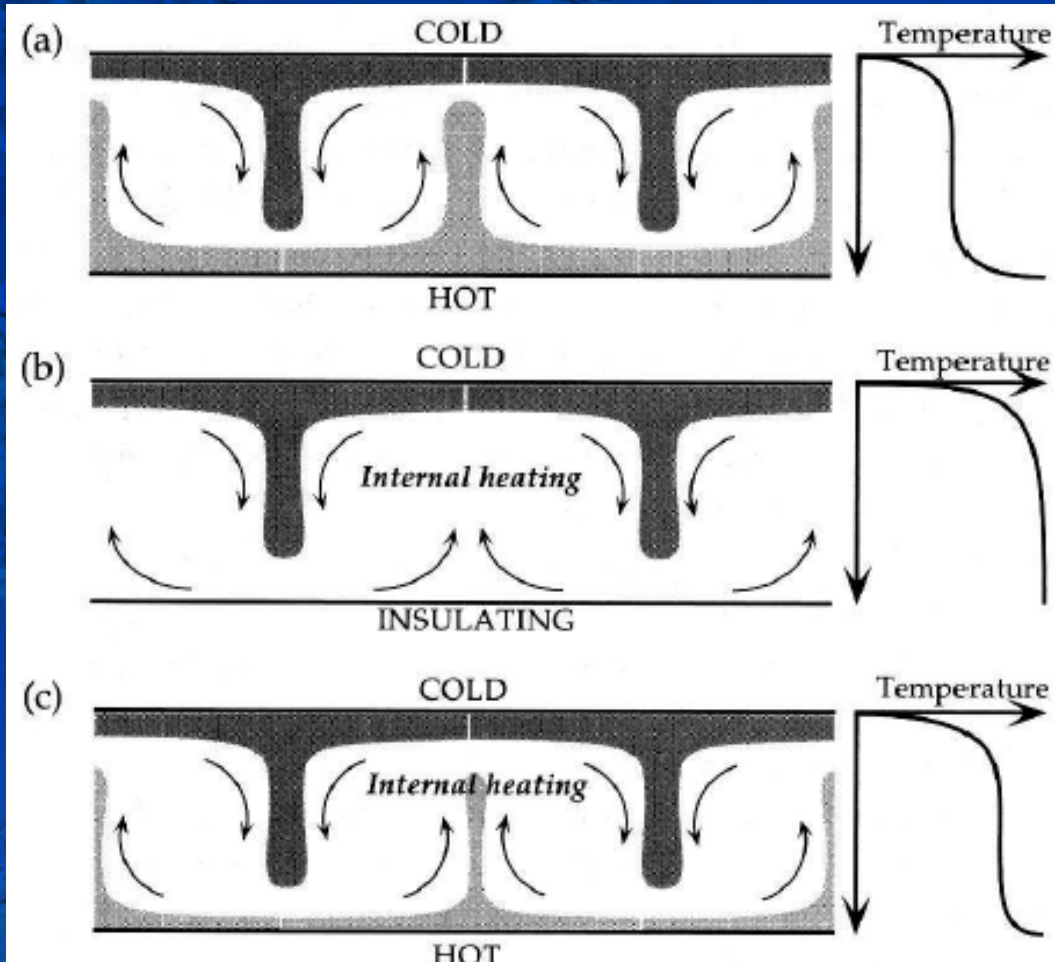
Context of heat flow variability

- Recent decrease in heat flow much larger than secular cooling, indicating periodic fluctuations
- Change in heat flow since 120 Ma such that Urey ratio at present may be an over-, rather than an underestimate
- Thermo-chemical scaling of heat transport may be required to avoid thermal catastrophe in Archean

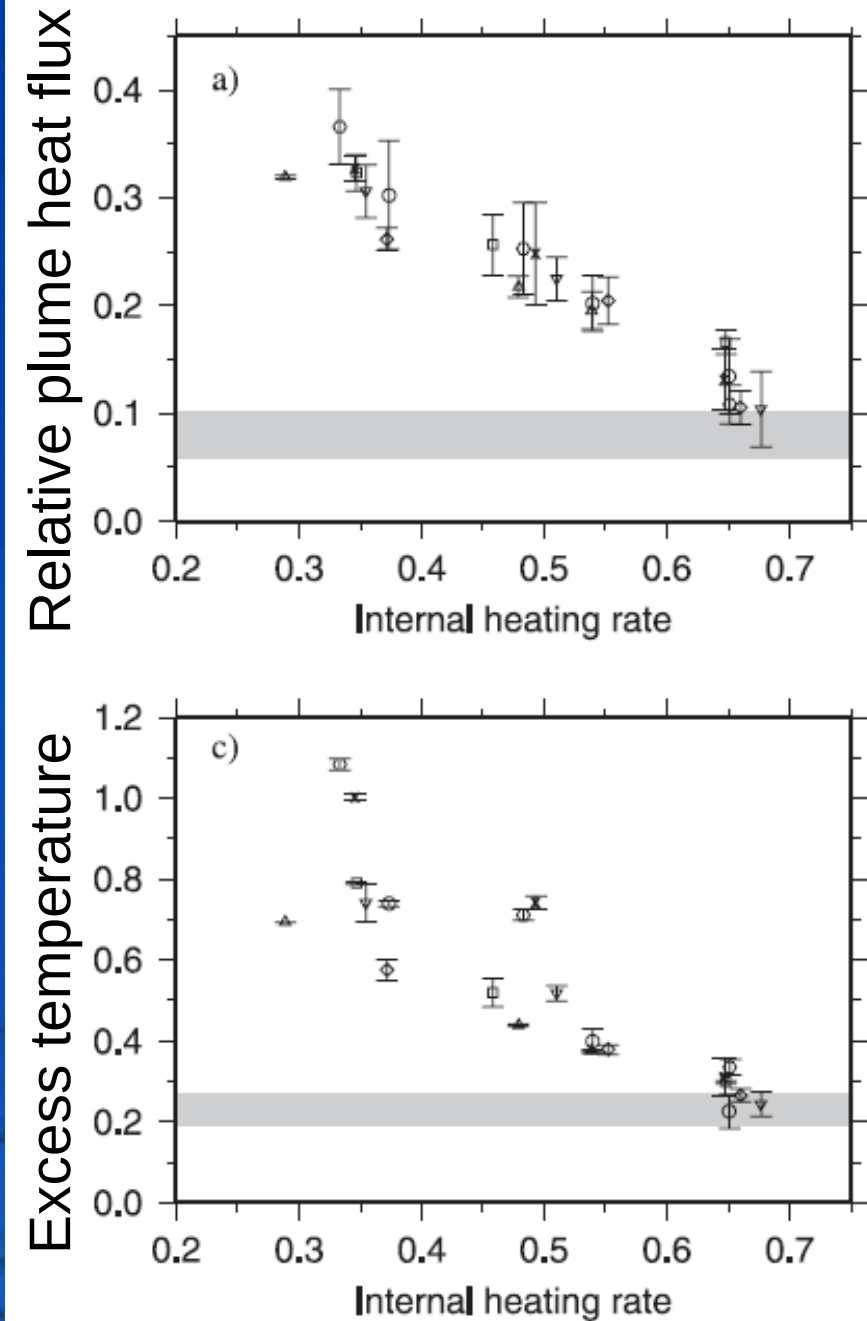
Constraints from dynamical plume models



Constraints on internal heating

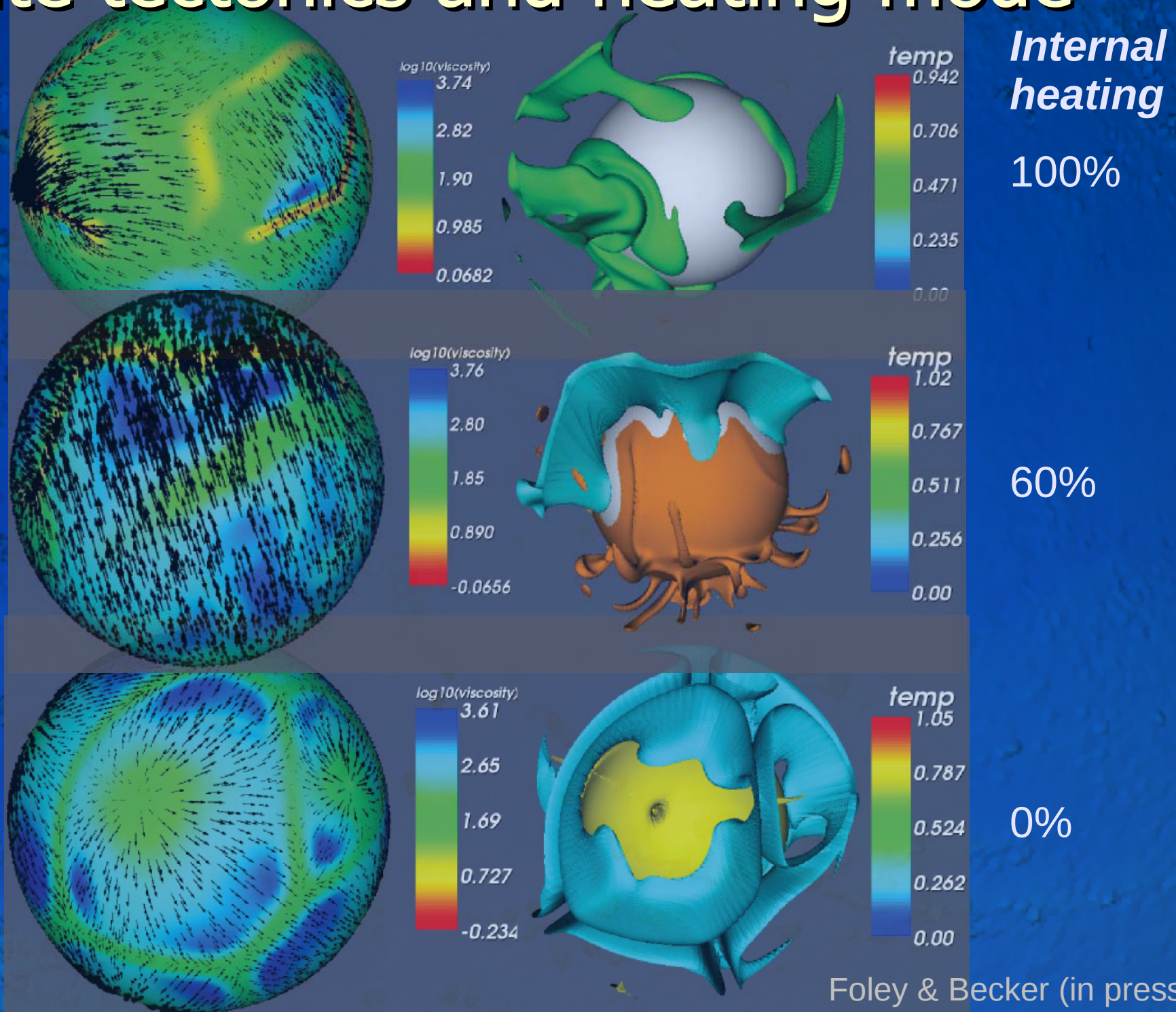


Davies (1999)



Zhong (2006); Leng and Zhong (2008)

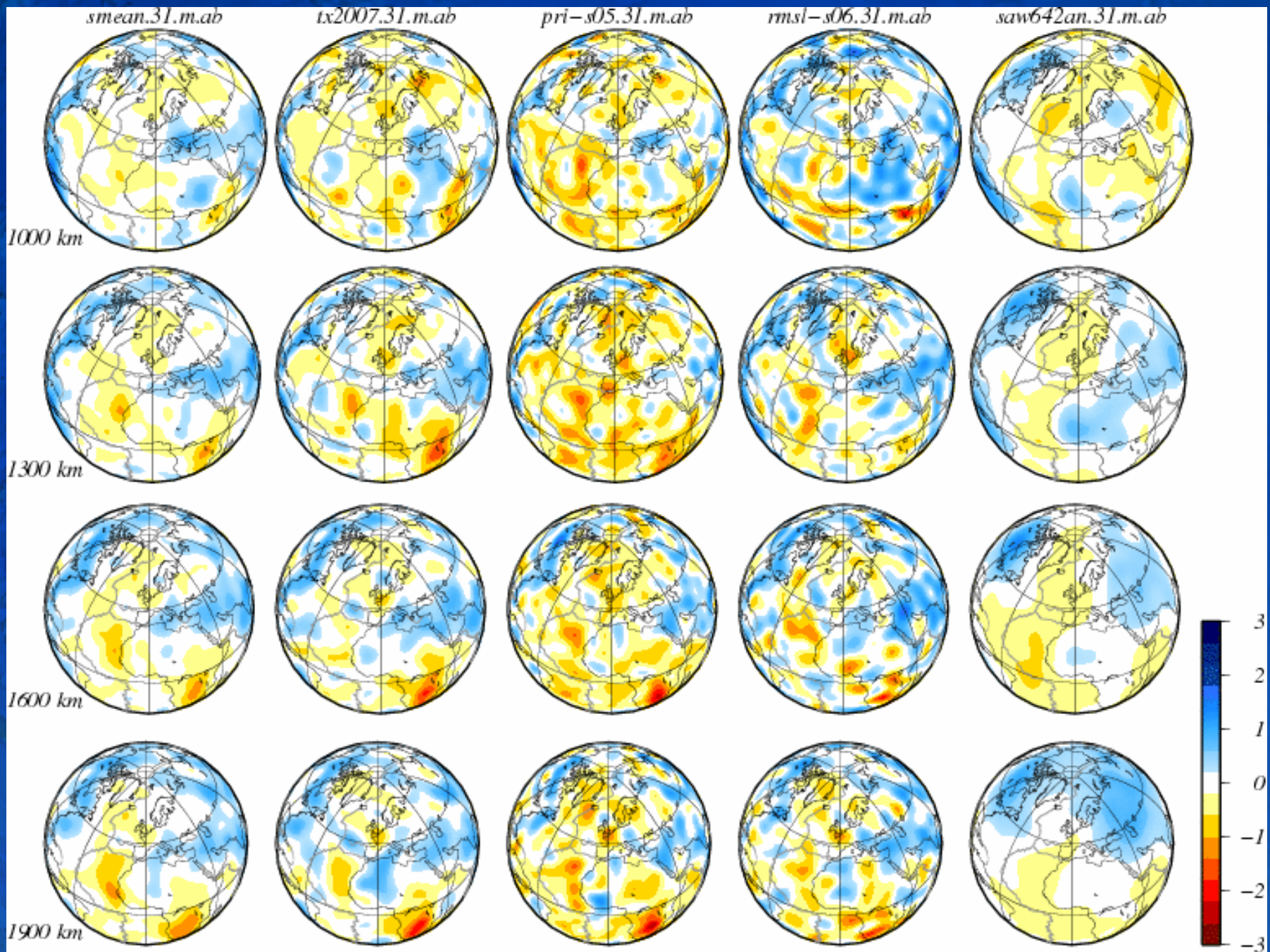
Plate tectonics and heating mode



cf. van Heck &
Tackley (2008)
Nakagawa et al.
(2009)
Yoshida (2008)

Foley & Becker (in press)

What is imaged in tomography?



$$\delta V_S = \Delta V_S / V_S [\%]$$

Evaluating the hotspot catalog

1. Azores
2. Balleny
3. Bowie
4. Cameroon
5. Canary
6. Cape Verde
7. Caroline
8. Cobb
9. Comores
10. Darfur
11. East Africa
12. East Australia
13. Easter
14. Eifel
15. Fernando
16. Galapagos
17. Guadelupe
18. Hawaii
19. Hoggar
20. Iceland
21. Jan Mayen
22. Juan Fernandez



23. Kerguelen
24. Lord Howe
25. Louisville
26. Macdonald
27. Marion
28. Marquesas
29. Meteor
30. New England
31. Pitcairn
32. Raton
33. Reunion
34. St. Helena
35. Samoa
36. San Felix
37. Socorro
38. Tahiti
39. Tasmanid
40. Tibesti
41. Trindade
42. Tristan
43. Vema
44. Yellowstone

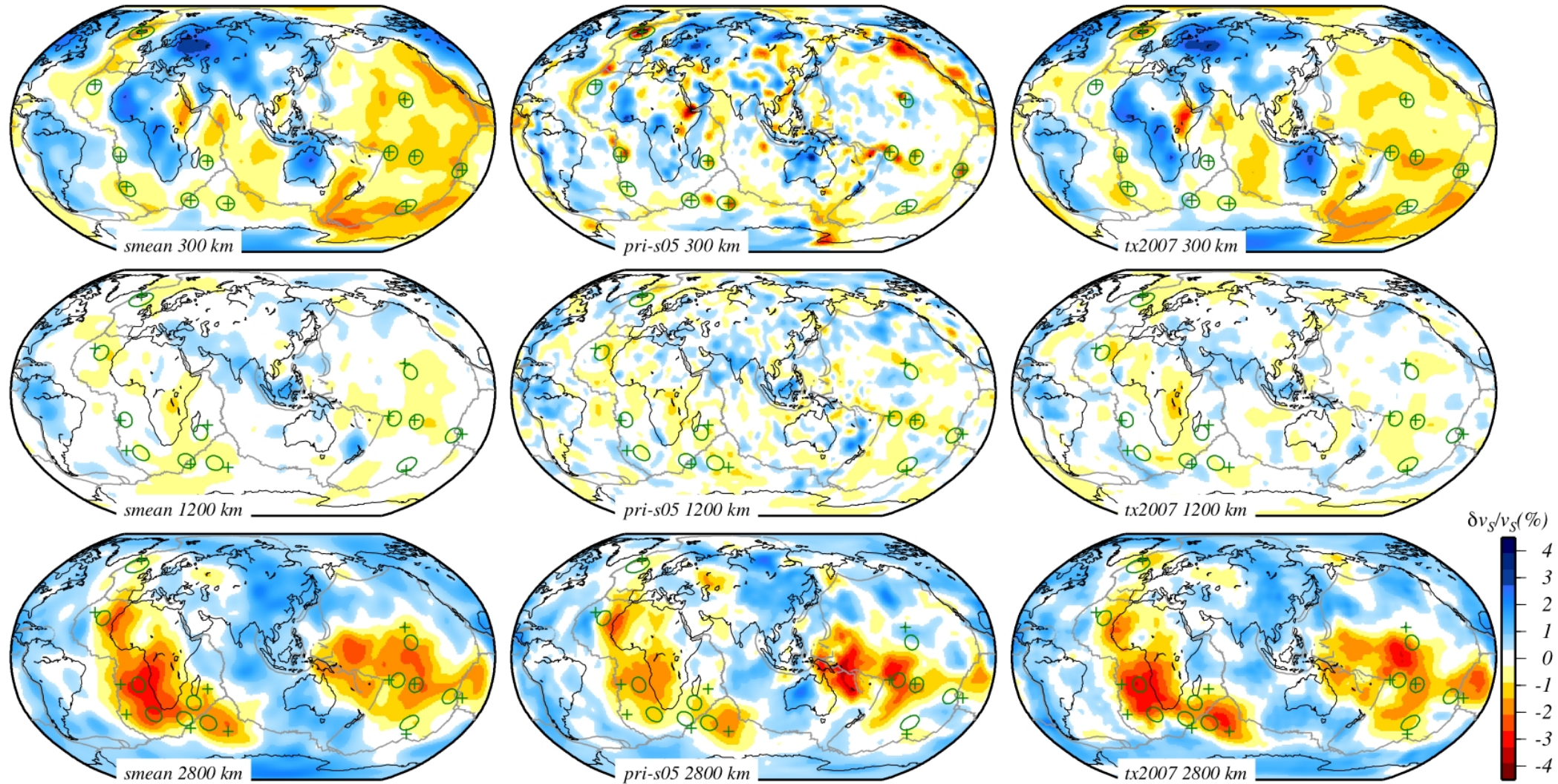
Circle radius scales with $\log(\text{buoyancy flux})$

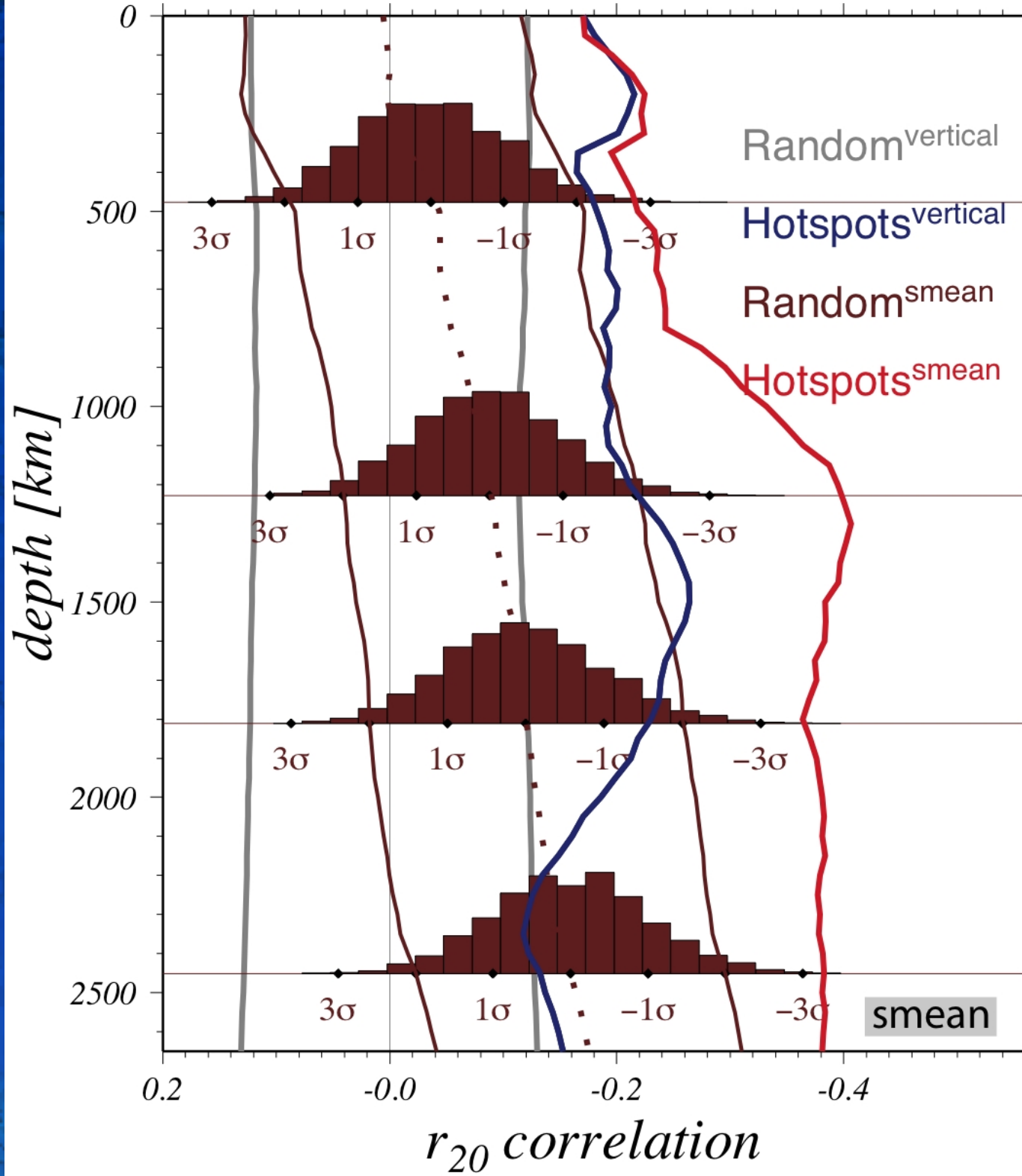
- Criteria for hotspot selection

- Two out of four:

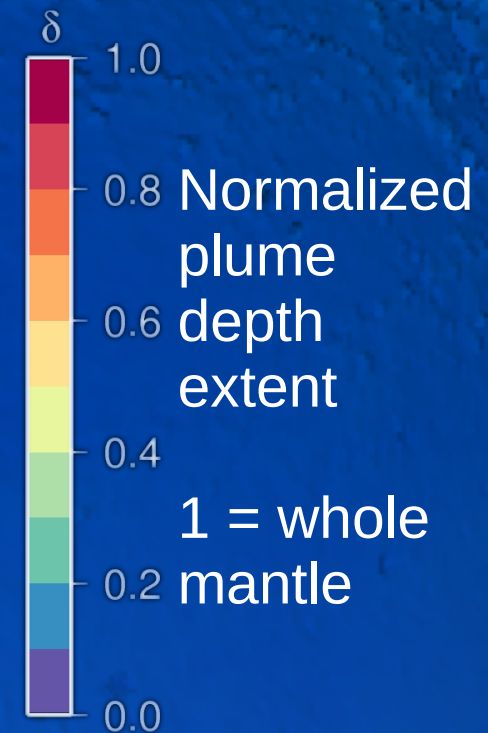
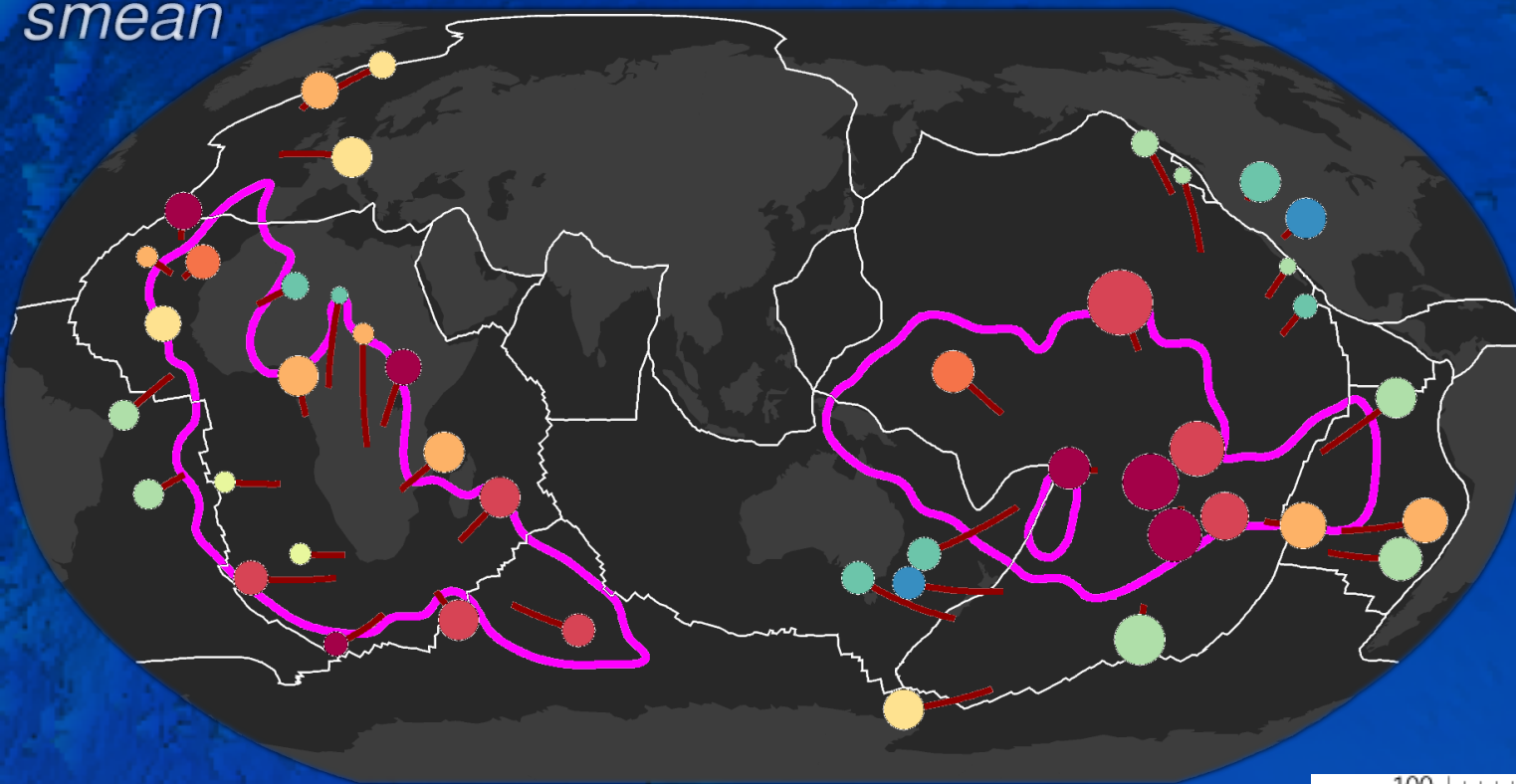
- Recent volcanism
- Swell or topography distinct
- Volcanic chain
- Flood basalt

S tomographic models; 12 likely deep plumes advection vs. no advection

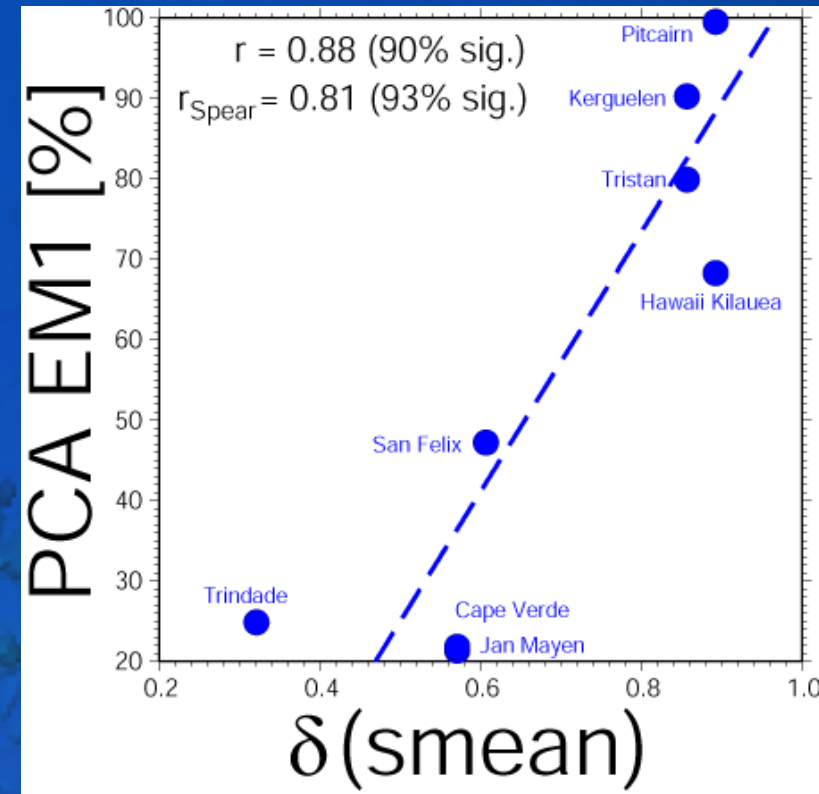




smean



- Many hotspots connected to deep plumes
- Plumes rise from within the large, low velocity provinces
- Free base motion preferred, no chemical pinning
- Conduit length correlates with OIB endmember EM1



Conclusions

- Some hotspots caused by deep plumes
- Correlations with tomography are statistically highly significant when conduit advection is taken into account
- Most deep plumes are on top of the Africa and South Pacific large low velocity zones
- Freely advected plume sources are preferred over fixed sources, no pinning on piles required
- Further exploration of petrological and geochemical data will help tighten plume constraints on heat flux